# THE OXIDATION AND SUBLIMATION OF GRAPHITE

# IN SIMULATED RE-ENTRY ENVIRONMENTS

J. W. Metzger
M. J. Engel
N. S. Diaconis

Space Sciences Laboratory
General Electric Company
Philadelphia, Pa.

N66-22255

FACILITY FORM 602

| (ACCESSION NUMBER) | (THRU) |
|---|---|
| 91 | |
| (PAGES) | (CODE) |
| CR 60395 | 8 |
| (NASA CR OR TMX OR AD NUMBER) | (CATEGORY) |

NASA   CR # 60395

## INTRODUCTION

As the state of the art of re-entry vehicle technology continues to advance the demands placed upon thermal protection systems for proposed missions become increasingly more severe. Whereas early designs in general incorporated plastics and re-inforced plastics as the ablative heat protection material, more recently the designer has given serious consideration to refractory materials for such applications. Certainly interesting candidates in this area are the graphites and many of the carbonaceous alloys.

While the choice of a vehicle heat shield material involves the consideration of many aspects of design requirements bearing on structural, fabrication, thermodynamic and signature criteria, in this paper we will concern ourselves only with the material thermochemical response to the re-entry environment. Although there are many types of graphitic materials, the choice to study a particular composition does not significantly compromise the investigation. Theoretical treatments in the literature (5, 6, 9, 10, 11) consider basically a carbon matrix and to this extent most graphites per se should be covered by such analyses. In this paper in which we will describe an experimental study of the oxidation and sublimation of such materials we will deal specifically with two types of graphite. These are ATJ, a fine grain commercial graphite produced by the National Carbon Company which has found application in numerous aerospace ventures and pyrolytic graphite, a highly anisotropic material produced by vapor deposition.

I

The information presented herein is a report of the current status of the study of graphite degradation in re-entry environments that has been in progress for a number of years at the Space Sciences Laboratory of the General Electric Co. An earlier report (ref. 8) presented some preliminary results on ATJ oxidation. The oxidation study which is now greatly augmented, and results of graphite performance while undergoing sublimation are the subject of this release. The experimental program is described, the data analysis techniques used to obtain the various correlations are presented and the comparison of the results with the theoretical treatments of Scala are shown.

# TECHNICAL APPROACH

## 1. Test Facilities

To obtain data over the broad range of temperature of interest in this study it was necessary to conduct the test program in more than one test facility. The major portion of the testing was conducted in a hypersonic arc tunnel in which environments were established for obtaining the rate controlled and diffusion controlled results (as defined by ref. 5). To obtain data in the sublimation regime a free jet arc facility was used.

All tests for the study of ATJ Graphite were conducted in the SSL Hypersonic Arc Tunnel. This system is comprised of a tandem Gerdien arc heater, a conical nozzle through which t e heated test gas is expanded into a continuously evacuated test section where the specimens are normally mounted, a diffuser aft of the test section, and a high speed mechanical vacuum pump. The tunnel is illustrated in Figure 1 and the arc heater in Figure 2.

The heater arrangement (Figure 2) is such that air is admitted tangentially to each Gerdien unit through vortex chambers located between the electrode housings and the plenum chamber. Valving in the air system provides a method of dividing the incoming air flows into two portions which are subject to close control. The greater portion of the air is bled from the system through exhaust ports in the electrode housings. In the course of its passage from the inlets to exhaust ports, the exhaust air carries with it the carbon products produced from

3

the graphite electrodes which would normally contaminate the test gas.

The remaining portions of the air admitted (which constitute the test gas) pass into the plenum from both sides, acquiring additional energy from the arc column. Contaminants, measured spectroscopically, constitute less than 100 parts per million of the test gas. The rotation induced in the air as it is admitted tangentially, is oppositely directed in the two halves of the arc, the opposed rotations tending to offset one another as the two flows enter the plenum and mix. The combined flow then passes from the plenum through the throat of the conical nozzle.

The nozzle is constructed in two parts, one of which is essentially an extension of the other. The up-stream section has an exit diameter of 1.2", while the extension, when added to the short nozzle, provides a nozzle of 5" exit diameter. All parts of the arc hardware and the nozzle are cooled with pressurized high velocity water in order to provide them with maximum service life.

The free jet facility used for the higher temperature testing is shown in Figures 3a and 3b. The major difference between this unit and the design used for the arc tunnel is in the plenum chamber, the basic shape of which has been changed from a large cylindrical section fo a small tee section. Whereas the former plenum diameter was 3 to 4 times the diameter of the vortex chamber constricting orifices, the orifice and plenum diameters in the present unit are equal. With this arrangement the stay time in the column

4

and plenum regions, and consequently the energy losses of the test gas, are significantly reduced. Test flows are sub-sonic and the model is located only a short distance downstream of the arc column in rather high stagnation enthalpy flows. Details of this facility and the arc tunnel can be found in Ref. 1 & 2 respectively. Whereas the ATJ studies were performed in the arc tunnel, only pyrolytic graphite testing was performed in the free jet.

2. Test Procedure

To measure the enthalpy of the test gas, a total calorimeter was used. This device (Figure 4) used in the arc tunnel consists of a cylindrical housing containing a labyrinth passage for the test gases. The adjacent walls are cooled with pressurized water to remove the heat transferred from the test gas. The calorimeter is affixed directly to the throat of the nozzle, located in the wall of the arc heater plenum. The heated test gas from the plenum is directed through the calorimeter where it transfers the bulk of this energy to the circulating water. The heat remaining in the gas as it leaves the calorimeter is monitored by a thermocouple and its mass flow rate is measured. Similarly, the temperature rise and mass flow of the circulating water are measured continuously during a test. Several thermocouples are mounted in the copper structure of the calorimeter to evaluate the heat "stored" in the walls. The test is continued until all reporting thermocouples equilibrate. The evaluation of the reported data, essentially a heat balance between the calorimeter elements and the test gas, results in a measure of the total heat content of the gas. Since it is estimated that there are some minor heat losses

5

which cannot be evaluated, the value of the enthalpy obtained will be slightly conservative. It should further be noted that the enthalpy determined is a "mean" of the distribution of energy across the jet; other measurements performed with a spectrograph also indicate enthalpy variations across the jet. In general these spectrographic measurements have recorded enthalpies about 6 percent higher than those obtained by total calorimetry.

Total calorimeter data were also obtained in the free jet facility using a similar approach to that used in the arc tunnel. The only difference involved the use of an adapter that fit into the test chamber to collect the test gases. This arrangement is shown in Figure 5.

Model measurements as part of the test program consisted of surface pressure, surface heat transfer and specimen surface temperature. The pressure values were obtained with pilot probes while the heat transfer was measured with transient calorimeter models corresponding to each of the test specimen configurations. A typical model calorimeter is shown in Figure 6. The calorimeter bodies were constructed from phenolic nylon, chosen for its low thermal conductivity and into each of these, a copper cylinder was inserted. A thermocouple attached to the back face of the copper slug recorded the rise in temperature in the copper during exposure. By confining the slug within a poor thermal conductor, the heat transfer rate was evaluated on the basis of a one-dimensional heat flow analysis although first order corrections for the heat loss from the slug were incorporated. One inch specimens were equipped with 1/4" diameter slugs while 1/4" bodies employed 1/8" diameter slugs.

To obtain heat transfer to a 1/16" diameter specimen, a rigid 60 mil copper rod was employed, and to minimize lateral heat input, the rod was coated with a 2 to 3 mil layer of RTV silicone rubber (a good thermal insulating material). The 1/16" calorimeter appeared to perform extremely well, but in order to provide a higher level of confidence in this technique, several calorimeters constructed from 1/4" diameter copper rod coated with a correspondingly thin RTV skin were tested. Results were closely comparable to the data obtained from the 1/4" phenolic nylon cylinders with 1/8" diameter copper inserts.

Several sizes of cylindrical specimens were involved in the acquisition of mass rate data. Sizes included diameters of 1/16", 1/4", 3/4" and 1". The configurations and dimensions of the specimens are shown in Figure 7a and 7b.

During the course of the arc tunnel program, various circumstances arose which warranted the introduction of several modifications to the specimens. Variations were introduced principally to the 1/4" diameter cylinders. It was found that during consecutive tests the surface temperatures of similarly constructed models equilibrated at temperatures that differed but little from one another. The results were thus confined to a relatively narrow range of temperatures. In order to extend the temperature range, variations of test specimens retaining the basic 1/4" diameter cylindrical shape were constructed (Figure 7c). Objectives sought by making such changes were (a) the alteration of the thermal conduction paths and (b) a change in the

7

heat storage volume for the specimen adjacent to the exposed surface. While the modified specimens did provide an increase in the range of surface temperatures obtained, the effects were not as pronounced as expected. However, for the same reasons, the 1/16" specimens were also tested in one other configuration (Figure 7b) in addition to the original. In this case, the increase in temperature range was also relatively small.

Measurements of surface temperature were made for each specimen while undergoing test. These were obtained with a recording two-color pyrometer employing two phototubes with maximum responses at different wavelengths. One tube has maximum response in the red portion of the spectrum, the other in the blue. The evaluation of the relative responses of the two tubes is interpreted as a color temperature. For models tested in the flow from the 5" diameter nozzle, the two color pyrometer views the specimens through a test section window. When the 1.2" diameter nozzle is employed, use is made of a special small port built into the arc heater mounting flange.

In the case of free jet testing, determination of surface temperature histories in general involved observing the test surface through both the ablation products and the high enthalpy air flows. As a check on the pyrometer measurements, model surface temperatures were also obtained by spectro-graphic means. Whenever extraneous radiators appeared in the pyrometer band width the spectrographic data were analyzed to determine temperature values.

# TEST RESULTS

### 1. Calorimeter Measurements

Total enthalpy of the test gas was measured for each of the two enthalpy levels at which the arc tunnel was operated and the results of the tests, using the total calorimeter have been summarized in Table 1. The evaluation process for data acquired from the calorimeter is a heat balance between a heat exchanger (the calorimeter) and the test fluid (air) after the system has reached steady state operation. Similar data for the free jet are presented in Figure 8 as a function of distance from the arc column of the heater. Model heat transfer results are shown in Figure 2.

### 2. Specimen Mass Loss

The mass loss data obtained from the cylindrical test specimens consisted of the difference in length resulting from exposure to the test environment. The differences were obtained from micrometer measurements taken before and after test. Length change at the stagnation point was used in preference to measured mass loss because it was not feasible to give accurate consideration to mass lost from the side wall of the cylinder. In the tunnel tests (where test times were quite long) the gross mass lost from a cylinder varied between two and three times the mass lost at the stagnation region of the specimen, as calculated from the length change using the following expression: $\Delta m = \rho A (\Delta \ell)$.

It is possible that some mass is driven from below the receding face of a specimen. Hence a comparative evaluation of mass rate based on length change and on mass loss over an area with protected side walls would be informative.

Provision for such a comparison was made on the one inch diameter specimens tested during the program. Since the diameter was sufficient, a small insert (1/4" diameter) was press fitted into a centerline cavity in the one inch specimens. Comparison of the results from weight and length measurements showed the weight loss generally to be about 5% greater.

A few specimens showed a measurable decrease in diameter as a result of side wall mass losses. This was especially noticed on the 1/16" diameter models. The net effect of such diametral decrease is a tendency for the heat transfer rate at the stagnation point to increase slightly ( $\dot{q}_o \propto 1/\sqrt{R}$ ). Hence, mass rates for the longer run times might be expected to be slightly larger. Data from the various runs in the tunnel are shown in Tables 3 to 8, and free jet results are indicated in Fig. 9.

3. Rate of Mass Loss

In order to present the results of the tests in a form comparable to the theoretical representation, it is necessary to obtain the mass rate of oxidation for incremental temperatures. While it may be possible in theory to evaluate mass rate as a continuous function of surface temperature from motion film records of the tests and time resolved surface temperature recordings, the relatively small dimensional change in the specimen puts a prohibitive penalty on the accuracy attainable. The technique used in this program employed a system of length and time differences.

Specimens were exposed to the test environment for various intervals of time, resulting in incremental differences in length change. The calculation of rate of mass loss per unit area proceeded from taking differences between length losses and times among the various specimens in the following manner:

$$\dot{m}_w = \rho \left( \frac{\Delta \ell_2}{\Delta t_2} - \frac{\Delta \ell_1}{\Delta t_1} \right)$$

The calculated mass loss rate is considered to represent that existing at the average temperature for the two test points evaluated, i.e.: $( T_1 + T_2 )/2$. Results are shown in Table 3 to 8 and Fig. 17.

4.  Surface Temperature

Typical surface temperature histories of specimens run in the arc tunnel obtained from the pyrometer measurements are shown in Figure 10. An example of similar measurements in the free jet are presented in Figure 9. Details of the data reduction techniques are available in Ref. 1 and 2.

## DISCUSSION OF RESULTS

1.  **Test Environments**

While the basic objective of the investigation was to establish the performance of the graphite materials over a broad range of surface temperature, the character of flows of electric arc heated facilities injects additional variables into the problem. Because of the high enthalpies generated in such facilities subsequent expansion of the gas in nozzles usually results in non-equilibrium conditions in the test section. In addition the magnitude of the flow properties is such that very low Reynolds number conditions result. As a result when considering the range of model sizes, model pressures and enthalpy values that were involved in this study, local model conditions ranged from continuum to near-free molecular values.

In order to determine the type of simulation performance which the arc tunnel facility could deliver, it was necessary to define the conditions of flow provided at different conditions of operation. Based on facility evaluation tests previously conducted in the Hypersonic Arc Tunnel (Ref. 3), a series of computations were made to determine the Reynolds number at the several test conditions. Alghouth the available spectrographic evidence indicates that the flow is in equilibrium as it leaves the plenum, sufficient evidence also exists that the flow freezes very rapidly in the vicinity of the throat of the nozzle (Ref. 4). Calculation of both the equilibrium and frozen flow expansions through the nozzle according to the treatment in Ref. 3 showed that while the local free

stream properties were quite different at the test locations, the Reynolds number for both frozen and equilibrium flow in the model stagnation region were of approximately the same magnitude. The variation ranged from 8-15% over the spread in Reynolds number. Consequently, when it was necessary to introduce a Reynolds number for tunnel tests, an average value was used for each set of conditions.

For the free jet facility, while higher enthalpy flows are generated, the greatly increased model pressure ($p_m \sim 1$ atm) encountered in the subsonic flow field provides the means whereby continuum flow criteria would apply.

2. Oxidation of Graphite

Once the numerous mass rate values had been computed (Tables 3-8) they were plotted as a function of reciprocal temperature with the objective of determining the activation energy (E) and the reaction rate coefficient ($k_o$) for the equation:

$$\dot{m} = k_o \sqrt{P_e} \; e^{-E/RT}$$

For pure reaction rate controlled oxidation, the given equation can be re-written in the form of the integrated Arrhenius equation, which requires that the natural log of $\dot{m}'$ vs. $1/T$ shall be a straight line.[1] It was not obvious from the examination of the data plotted in this form (Fig. 11) that this was the case.

---

1. In this report, direct reference to unadjusted mass rate data employs the symbol $\dot{m}'$ ; corrected data is denoted by the conventional $\dot{m}$.

Since it was fully expected that some of the specimens would have been oxidized under conditions of diffusion control a departure from a linear plot was not surprising. The deviation obtained tended to confirm the presence of the diffusion controlled activity. Coupled with the scatter of the data points, the narrow range of mass rates for which linearity might be assumed made it difficult to plot a straight line which could be considered properly representative of the reaction. In lieu of an estimated slope of great uncertainty it was decided that a value would be chosen which was typical for graphite materials. The slope is a measure of the activation energy. Consultation with the available literature led to a choice of 44.0 kilocalories as a good representative value. A straight line with this slope was constructed to pass through the bulk of data points estimated to be predominantly reaction rate controlled. Based on the constructed line, the reaction coefficient was determined:

$$k_o = 4.42 \times 10^5 \text{ lb/sec.ft.}^2 \text{ atm}^{1/2}$$

The equation for the reaction rate oxidation of graphite was then substituted along with the theoretical diffusion controlled oxidation correlation of Ref. 5

$$\dot{m}_D = 6.2 \times 10^{-3} \frac{P_e^{1/2}}{R_B^{1/2}} \quad \frac{\text{lb}}{\text{ft.}^2\text{-sec}}$$

into the transition regime relation presented in Ref. 6

$$\dot{m} = \frac{1}{\left[\dfrac{1}{\left(\dot{m}_R\right)^2} + \dfrac{1}{\left(\dot{m}_D\right)^2}\right]^{1/2}}$$

14

Curves were computed for each type specimen and test condition (see Appendix B) and the results are shown in Fig. 11. It is evident that in the diffusion controlled regime (constant mass rate) the data points are high with respect to the theory. Because the test facility provided environments which were characterized by non-continuum flows, these differences were expected.

The theory developed by Scala (Ref. 5) to describe the oxidation of graphite was based on flow of high Reynolds number. In Ref. 2 that theory is extended to regions of low Reynolds number and to molecular flow. The extension provides that data of both rate controlled and diffusion controlled oxidation must be adjusted in order to compare it with high Reynolds number continuum based theory, or vise versa. In their final forms, the modifications consist of applying a Stanton number ratio correction factor to data in the diffusion controlled regime or an effective pressure ratio correction factor to data in the reaction rate controlled regime. Both these factors are functionally de-pendent upon the Reynolds numbers corresponding to the test flow conditions. From calculated nominal values of Reynolds number per foot, corresponding to the various test conditions, the shock Reynolds number for each model was determined. The appropriate correction factors for either oxidation process were then obtained from the graph of Stanton number ratio vs. $Re_s$ (Figure 12) or the graph of $\left[ P_{O_2} / .21 \rho_\infty V_\infty^2 \right]$ vs. $Re_s$ (Figure 13).* Data point values must be divided by the correction factors determined from these graphs.

---

* Both Fig's. 12 and 13 are reprinted from Ref. 2 where they are Fig's. 22 and 23

In examining the mass rate plotted against $1/T$, it may be seen that many of the points lie near the transition region of the theory curves. For these points, correction factors are needed which are intermediate between those appropriate for diffusion control and for rate control. To accomodate these points, the theoretical expressions were examined and the contribution of each factor was weighted for each point in the transition region. Refer to Appendix C. Once the appropriate correction factors were determined for all regions containing data, they were applied, each to its corresponding datum point, to determine the mass rates in terms of Scala's original theory (Tables 3-8).

A second graph of $\dot{m}$ vs. $1/T$ was prepared showing the adjusted data over-plotted on the theoretical curves (Figure 14). It may be seen that the diffusion controlled data are decreased and conform reasonably well to the predicted performances. In general, the rate data are increased in value, although the changes in position with respect to the theory curves are less pronounced because of the near-vertical slope of the reaction rate portions of the curves.

It is interesting to note that when the data are corrected, the shift of reaction rate data may be sufficient to warrant the construction of a new, displaced slope for the activation energy and alteration of the weighting factors in the transition region. Extrapolated to its extremity, this becomes an iterative process which ceases when the required degree of accuracy has been attained. In the present case, the scatter of the data points is sufficient to make further approximations unjustified.

Having shown that the mass loss rate data does indicate reasonable concurrence with the theory, the final step was to prepare a plot of the data normalized with respect to pressure and specimen radius. However, it was evident that data corrected to correspond to the theory curves would tend toward a more crowded pattern. In order to better examine the relative correspondence of theory and experiment for the individual test conditions, the theory curves were modified for $Re_s$ effects as the correction factors indicated, while the original mass rate data were normalized with respect to pressure and body radius only (Tables 3-8). The results were plotted ($\dot{m}' = \sqrt{R_B/P_e}$ vs $T_w$; Figure 15) to provide a clearer picture of the degree to which theory and experiment agree.

Finally, the appropriate correction factor was applied to each datum point normalized with respect to pressure and specimen radius (Tables 3-8), and the computed results were incorporated into a plot ($\dot{m}\sqrt{R_B/P_e}$ vs. $T_w$; Figure 16) in which the theory curves remain in the form calculated from the unmodified continuum theory. The theoretical curves predict a dependency of data on the body size only in the reaction rate controlled regime but independence with respect to both pressure and body size in the diffusion controlled regime. The methods employed in reducing the data are described in detail in Appendix C.

Aside from the scatter of data it may be seen that there is indeed a trend which places the 1/4" specimen data between the majority of one inch and of

1/16" specimen data. In addition, the data for all three model sizes are in approximately the proper relation to one another as predicted by the theory. Note also that the $6.2 \times 10^{-3}$ lb/ft$^{3/2}$sec.atm$^{1/2}$ plateau is placed in the midst of the data points corresponding to diffusion controlled oxidation.

The experimental results assuredly concur with the theory when a mean value of the data is considered.

3.   Sublimation of Graphite

As mentioned earlier the free jet tests were not conducted with ATJ graphite, but rather with pyrolytic graphite. Even though a different form of graphite is being used the data obtained are characteristic of diffusion controlled and sublimation thermochemical degradation and theoretically this should be independent of the crystalline structure of the material. From the data shown in Fig. 9a and b one can observe the severity of the test environment produced in the free jet. This is indicated by the attainment of sublimation temperature in less than one second (Fig. 9a). Once that plateau is reached, the temperature remains constant for the remainder of the test time. The mass loss data, computed from the change in the length of the specimen at the stagnation point and the density of the material, shows essentially a linear variation with time as expected. The small drop in temperature at the longer times is accompanied by a lower rate of mass loss. These effects are attributed to a reduced heating rate caused by the models becoming slightly concave during a longer run. The low surface temperature during the first second of exposure is responsible for the failure of an extrapolated straight line through the data to go through the origin. Similar results

18

are shown for the lower enthalpy flow in Fig. 9b. The material again heats up very rapidly except that the level of temperature attained is considerably lower. From the mass rate value the correlation $\dot{m}\sqrt{R_B/P_e}$ is established and these results are shown in Fig. 17. The three points shown correspond to the mass loss rate lines - best fit and high and low uncertainty limits - shown in Fig. 9. The temperature spread is due to the maximum uncertainty in fitting the experimental spectral intensities to theoretical spectral distributions (temperature determined by spectroscopy).

Before the data can be plotted on Fig. 17, however, the value of $R_B$ must be chosen. Since the theoretical relations have been developed for a Newtonian pressure distribution on a sphere and the present experiments have been conducted in a subsonic flow on a flat faced cylinder, we must account for this difference in comparing experiment with theory. In essence, an effective radius for an equivalent body in a Newtonian flow field has been established and used to compute the correlation parameter for the experimental data.

The determination of an appropriate value for the effective radius (or the model stagnation point velocity gradient) in a subsonic high enthalpy flow field when the model size is of the order of the test jet is not a straightforward problem. Analyses are available in classical hydrodynamics dealing with the impingement of streams on flat plates and discs; however, there appears to be no satisfactory analytical way to account for interference from the walls of the small test chamber. Also, accurate measurement of surface pressure gradients are extremely difficult in the severe test environments.

Because of these problems, an effective radius was determined by in-
ference from the ATJ data since these have been shown to be in good agreement
with the theory in the diffusion controlled regime. It was assumed that the
theoretical diffusion controlled mass parameter value $\left( \dot{m} \sqrt{R_B/P_e} \right)_D$ was
also correct for the free jet tests and a radius calculated using the test data.
This gave $R_B = 2.4 \, R_B$ geom.

A second experimentally based method can also be used to determine an
effective $R_B$ value. This approach uses the measured stagnation point con-
vective heat transfer and enthalpy values and infers an $R_B$ value by comparing
results with theory. Using the theoretical results of Scala and Baulknight (7)
and the nominal test conditions ( $\bar{h} = 490 \, RT_o$, $P_e = 1$ atmosphere, $\dot{q}_c = 2050$
BTU/ft$^2$-sec) we get $R_B = 2.9 \, R_B$ geom.

These two $R_B$ values are not greatly different; however, we have used the
first value, instead of an average, for two reasons. First, a 21% uncertainty
in $R_B$ is indicative of only about a 10% uncertainty in heating rate. This is no
better than should be expected in this type of test environment. Second, the use
of an experimental measurement of the same type as that used in obtaining the
data of interest (graphite material loss rate) to establish the experimental base
for deduction of an effective $R_B$ eliminates those sources of potential error
peculiar to a calorimeter measurement.

The experimental results in Fig. 17 are compared with the sublimation
theory of Scala and Gilbert (6). Because of the scatter in the temperature data

( $\pm$ 5%) it was not possible to make a more careful evaluation. Even though the stated temperature variation is within general experimental accuracy, a further improvement will be required due to the extreme sensitivity of material degradation to temperature in the sublimation region. As a general comment however, one might say that the theory and experiment yield comparable results.

## REFERENCES

1.) Diaconis, N.S., Weber, H.E., Warren, W.R.; Technique for Severe Radiative and Convective Heating Environments for Materials Evaluation; Pres. 3rd Hyper. Tech. Sym. - March 17-18, 1964 Denver, Col. (Also GE MSD TIS R64SD24, March, 1964)

2.) M.J. Engel, et al, The Effects of Atmospheric Re-Entry on Graphitic Particles, Final Rept. Contract SNPC-10, SNPO, Cleveland, Ohio, January, 1964

3.) Warren, W.R., Diaconis, N.S., Air Arc Simulation of Hypersonic Environments, GE TIS R62SD25; April, 1962, Pres. Int'l Hypersonics Conf. M.I.T., Cambridge, Mass., August, 16-18, 1961.

4.) Eschenroader, A.Q., et al, "Exact Solutions for Non-Equilibrium Expansions of Air With Coupled Chemical Reactions", CAL Rpt. No. AF-1413-A-1, AFO SR 622, May, 1961.

5.) Scala, S.M., The Ablation of Graphite in Dissociated Air, Part I, Theory, IAS Paper No. 62-154, Thirtieth Nat'l. Summer Mtg., June 1962 (also GE MSD TIS R62SD72, September, 1962).

6.) Scala, S.M. and Gilbert, L.M.; The Sublimation of Graphite at Hypersonic Speeds; GE MSD TIS R64SD55, August, 1964.

7.) Scala, S.M. and Baulknight, C.W.; Transport and Thermodynamic Properties In a Hypersonic Laminar Boundary Layer, Part 2, Applications; ARS Journal, Vol. 30, No. 4, pp 329-336, April, 1960.

8.) Diaconis, N.S., Gorsuch, P.D. and Sheridan, R.A., The Ablation of Graphite In Dissociated Air, Part 2, Experiment; Pres. Thirtieth IAS Nat'l. Summer Mtg. June, 1962, ( also GE MSD TIS R62SD86, September, 1962).

9.) Denison, M.R. and Dooley, D.A.; Combustion In The Laminar Boundary Layer of Chemically Active Sublimators, Aeronutronic Systems Rept. U-110, Sept., 1957.

10.) Moore, J.A. and Zlotnick, M.; Combustion of Carbon in An Air Stream, AVCO, RAD-TR-9-60-32, December, 1960.

11.) Welsh, W.E., Jr. and Chung, P.M.; A Modified Theory for the Effect of Surface Temperature On the Combustion Rate of Carbon Surfaces In Air, Proc. of 1963 Ht. Trans. and Fluid Mechanics Inst., Calif. Inst. of Tech., Calif., June, 1963 Stanford Univ. Press pp 146-159.

## APPENDIX A

### List of Symbols

| | |
|---|---|
| ATJ | ATJ grade graphite |
| C | diffusion-controlled mass transfer constant |
| $C_H$ | Stanton number |
| E | activation energy |
| f | distribution function; fractional ratio |
| $F_m$ | mass transfer rate modification factor |
| $h_s$ | stagnation enthalpy |
| $k_o$ | specific reactivity coefficient |
| $\dot{m}$ | mass transfer rate of ablating (or oxidizing material) per unit area |
| $\dot{m}'$ | unadjusted mass transfer rate per unit area |
| n | number density; reaction order |
| N | ratio, $\dot{m}_R / \dot{m}_D$ |
| $P_{O_2}$ | pressure of oxygen |
| $P_e$ | stagnation pressure |
| $\dot{q}$ | heat transfer rate per unit area |
| $R_B$ | radius of body |
| Re | Reynolds number |
| $Re_s$ | shock Reynolds number |
| $RT_o$ | enthalpy at ambient conditions (33.86 Btu/lb) |
| t | time |
| T | temperature |
| $\Delta$ | difference or change |
| $\rho$ | density |

A-1

Subscripts

| | |
|------|----------------------|
| B.L. | boundary layer |
| D | diffusion control |
| eff. | effective |
| ff | flat face |
| F.M. | free molecular |
| H.R. | high Reynolds number |
| L.R. | low Reynolds number |
| R | reaction rate control |

## APPENDIX B

### DERIVATION OF COMBINED
### THEORETICAL-EMPIRICAL EQUATIONS

In order to graphically represent the combined theoretical-empirical

mass loss performance of the materials studied in this program, the

following expressions were employed:

$$\text{Let } \dot{m}_R = k_o \sqrt{P_e} \; e^{-E/RT} \qquad \text{represent rate controlled} \quad (1)$$

mass loss

$$\text{Let } \dot{m}_D = C \sqrt{P_e/R_B} \qquad \text{represent diffusion con-} \quad (2)$$

trolled mass loss

$$\text{Let } \dot{m} = \frac{1}{\left[ \left(\frac{1}{\dot{m}_R}\right)^2 + \left(\frac{1}{\dot{m}_D}\right)^2 \right]^{1/2}} \qquad \begin{array}{l}\text{represent transition} \quad (3) \\ \text{from rate controlled} \\ \text{to diffusion controlled} \\ \text{mass loss}\end{array}$$

Substitution of (1) and (2) into (3) yields, after some algebraic re-arrange-

ment,

$$\dot{m} = \frac{k_o \sqrt{P_e}}{\left[ e^{2E/RT} + \left(\frac{k_o}{C}\right)^2 R_B \right]^{1/2}} \qquad (4)$$

from which the curves on Figures 32, 33, 52 and 53 were calculated.

Further, if one lets

$$f_1 = \text{fractional ratio of Stanton No.}$$

$$f_2 = \text{fractional ratio of effective pressure ratio}$$

replacing $\dot{m}_D$ by $f_1 \dot{m}_D$ and $\dot{m}_R$ by $f_2 \dot{m}_R$ in eq. (3) one may derive

$$\dot{m}' = \frac{f_2 k_o \sqrt{P_e}}{\left[ e^{2E/RT} + \left(\frac{f_2 k_o}{f_1 C}\right)^2 R_B \right]^{1/2}} \qquad (5)$$

-B-1

For the normalized mass loss rates a similar series of substitutions gave

$$\dot{m} \sqrt{\frac{R_B}{P_e}} = \frac{k_o e^{-E/RT}}{\left[\frac{1}{R_B} + \left(\frac{k_o}{C}\right)^2 e^{-2E/RT}\right]^{1/2}} \quad (6)$$

for curves expressed in terms of the theory (Figures 35 and 54).

The theory curves modified to correspond to data points acquired in their actual environments were determined from

$$\dot{m}' \sqrt{\frac{R_B}{P_e}} = \frac{f_2 k_o e^{-E/RT}}{\left[\frac{1}{R_B} + \left(\frac{f_2 k_o}{f_1 C}\right)^2 e^{-2E/RT}\right]^{1/2}} \quad (7)$$

This arrangement was used to relate the ATJ data more clearly with respect to the theory (Figure 34).

In order to correlate data points with the theory curves (as represented by eq'ns. (4) and (6), a slightly different approach was used in which it was necessary to determine a weighting factor for each test point. To establish this factor a tabulation of $\dot{m}$ was made for conditions under which the ratio of $\dot{m}_R/\dot{m}_D$ assumed particular values. For each material, the ratio

$$\frac{\dot{m}_R}{\dot{m}_D} = \frac{k_o \sqrt{R_B} e^{-E/RT}}{C}$$

was evaluated and the appropriate range of temperatures was determined for each size specimen. The extent to which each mass rate $(\dot{m}_D, \dot{m}_R)$

contributed to the combined mass rate ($\dot{m}$) for the corresponding condition

was evaluated as the weighting factor for the datum point. See Appendix C.

For a given set of nominal operating conditions, the factors $f_1$ and

$f_2$ were dependent upon the shock Reynolds number and hence were

treated as constants to which the weighting factors were applied.

In the preceding equations:

| | ATJ Graphite |
|---|---|
| $k_o$ (lb./sec. -ft$^2$-atm$^{1/2}$) | $4.42 \times 10^5$ |
| E (cal/mole) | $44.0 \times 10^3$ |
| C (lb./sec. -ft$^{32}$-atm$^{1/2}$) | $6.2 \times 10^{-3}$ |

## APPENDIX C

### DISCUSSION AND PRESENTATION OF SAMPLE CALCULATIONS
### REGARDING DATA REDUCTION

To illustrate the process of reducing mass rate data in the experimental

program, the results of two test runs are presented and carried through

each of the calculations used. Where necessary, details of the specific

procedures are expanded.

Consider the results of runs 521 and 560 on 1/16'' diameter ATJ

graphite mass rate specimens (Table 15):

| Run No. | Time sec. | Length Chg. inches | Mass Loss $lb/ft.^2$ | Mass Rate $lb/sec.ft.^2$ | Ave. Surf. Temp. $^{o}K$ |
|---|---|---|---|---|---|
| 560 | 250 | .0750 | .6751 | --- | --- |
| 521 | 60 | .0166 | .1494 | --- | --- |
| | 190 | .0584 | .5257 | $2.77 \times 10^{-3}$ | 1515 |

Difference in time and mass loss between the two runs at the same

test conditions result in one mass rate data point at an average surface

temperature $(T_w)$ of $1515^{o}K$.

$$\dot{m}' = \frac{\Delta m}{\Delta t} = \frac{\rho \Delta \ell}{12 \Delta t} = \frac{108 \times .0584}{12 \times \Delta t} = \frac{.5257}{\Delta t}$$

$$\dot{m}' = 2.77 \times 10^{-3} \ lb/sec.ft.^2 \ (\text{data pt. Figure 32, sym. } \bullet)$$

Other data, useful later in the computations are:

Reynolds number per foot $= 520$ ft.$^{-1}$

Reynolds number, $Re_s = 520 \times \frac{1}{16} \times \frac{1}{12} = 2.7$

Effective radius, $R_B = 2.46 \times \frac{1}{32} \times \frac{1}{12} = 6.41 \times 10^{-3}$ ft.

Model stagnation pressure, $P_e = 7.70 \times 10^{-3}$ atmos.

The individual data points ($\overset{\bullet}{m}{}'$) were located on an Arrhenius plot ($\overset{\bullet}{m}{}'$ vs $1/T$, Figure 32). Collectively, they were used to establish a reaction rate slope from which the specific reactivity ($k_o$) and activation energy (E) of the ATJ graphite were evaluated. The values obtained were expressed in a reaction rate equation, which when coupled with the theoretical expression for diffusion controlled activity by the transition equation, provided a single equation (Appendix B) from which "theoretical" performance curves were evaluated. These were overplotted on the Arrhenius graph (Figure 32).

The computed mass rates are for data acquired in regimes other than those of high Reynolds number, for which the original theory was derived. Hence experimental data have to be modified to correspond to the theory. The value of the modification factor ($F_m$) depends on the degree to which oxidation is rate controlled or diffusion controlled. The plotted theory curves depict graphically a qualitative sense of the contribution of each process and indicate that the modifying factor required by either process must be weighted against that of the other process depending on their relative predominance for a given test point. The following discussion constitutes the basis for obtaining a "weight" applicable to a given data point. Every point was individually weighted.

$$\dot{m} = \cfrac{1}{\left[\cfrac{1}{\dot{m}_D{}^2} + \cfrac{1}{\dot{m}_R{}^2}\right]^{1/2}} \qquad \text{(Transition equation, Sec. IIC, eq'n 30)}$$

Let $N = \dot{m}_R / \dot{m}_D$ $(0 \leq N \leq \infty)$. Then

$$\dot{m} = \cfrac{1}{\left[\cfrac{1}{\dot{m}_D{}^2} + \cfrac{1}{N^2 \dot{m}_D{}^2}\right]^{1/2}} = \cfrac{\dot{m}_D}{\left[1 + \cfrac{1}{N^2}\right]^{1/2}}$$

Divide both sides by $\dot{m}_D$

$$\cfrac{\dot{m}}{\dot{m}_D} = \cfrac{1}{\left[1 + \cfrac{1}{N^2}\right]^{1/2}} = \cfrac{N}{\left[N^2 + 1\right]^{1/2}}$$

The ratio gives $0 \leq \dfrac{\dot{m}}{\dot{m}_D} \leq 1$, which has the virtue of excluding explicit use of mass rates in the right hand member. For any given value of N, the contributing mass rates are $\dot{m}_D$ and $\dot{m}_R = N\dot{m}_D$.

The relative contribution of either process can be seen in the expression:

$$\cfrac{\dot{m}}{\dot{m}_D} = \cfrac{1}{\left[1 + \cfrac{1}{N^2}\right]^{1/2}}$$

If $\dot{m}_R$ is N times $\dot{m}_D$ (as postulated), it contributes $\dfrac{1}{N^2}$ toward the value of $\dot{m}$ when $\dot{m}_D$ contributes unity, relative to it. Their total contribution is $1 + \dfrac{1}{N^2}$ and their fractional contributions are

$$\text{for } \dot{m}_R; \qquad \cfrac{1/N^2}{1 + 1/N^2} = \cfrac{1}{1 + N^2}$$

$$\text{for } \dot{m}_D; \qquad \cfrac{1}{1 + 1/N^2} = \cfrac{N^2}{1 + N^2}$$

Note that for $N \to \infty$, ratio $\dot{m}/\dot{m}_D \to 1$. (diff. control)

$\quad\quad\quad\quad N \to 0$, ratio $\dot{m}/\dot{m}_D \to N$ (rate control)

$\quad\quad\quad\quad N = 1$, ratio $\dot{m}/\dot{m}_D \to \frac{1}{2}\sqrt{2}$ (equal control)

Numerical solutions follow:

$$\frac{\dot{m}_R}{\dot{m}_D} = N = \frac{k_o \sqrt{P_e}\ e^{-E/RT}}{\sqrt{C\ \dfrac{P_e}{R_B}}} = \frac{k_o \sqrt{R_B}\ e^{-E/RT}}{C}$$

where C is the diffusion control level in $lb/ft.^{3/2}$-sec-atm$^{1/2}$

Then $\quad N = \dfrac{4.42 \times 10^5\ (e^{-22150/1515})}{6.2 \times 10^{-3}\ (384)^{1/2}}$

$\quad\quad\quad N = \dfrac{7.15 \times 10^7}{19.6\ (2.705 \times 10^6)}$

$\quad\quad\quad N = 1.35$

Thus, the contributed fractions are

$\quad\quad$ for $\dot{m}_R$; $\quad \dfrac{1}{1 + N^2} = .335$

$\quad\quad$ for $\dot{m}_D$; $\quad \dfrac{N^2}{1 + N^2} = .645$; where $.645 + .355 = 1.00$

For the 1/16" diameter mass rate models, $Re_s = 2.7$; using this value one obtains a Stanton Number ratio ($f_1$) of 0.60 (Figure 22) for the diffusion controlled oxidation and an effective pressure ratio ($f_2$) of 0.44 (Figure 23) for rate controlled oxidation.

Then

$$\frac{f_1 N^2}{1 + N^2} + \frac{f_2}{1 + N^2} = F_m; \text{ Weighted Modifying Factor}$$

$$0.60 (0.645) + 0.44(0.355) = 0.543$$

The originally calculated data point can now be modified, $\dot{m}'/F_m = \dot{m}$,

thus, $\dot{m} = \dfrac{2.77 \times 10^{-3}}{0.543} = 5.22 \times 10^{-3}$ lb/sec.ft.$^2$ (data pt., Figure 33)

giving the value of the mass rate corresponding to that predicted by the

original theory.  The value of $\dot{m}'$ or of $\dot{m}$ may be normalized with respect

to body radius and pressure and plotted against surface temperature (for

this pt., $T_w = 1515^\circ$K).

Therefore,

$$\dot{m}'\sqrt{\frac{R_B}{P_e}} = 2.77 \times 10^{-3} \left(\frac{6.41 \times 10^{-3}}{7.70 \times 10^{-3}}\right)^{1/2}$$

$$= 2.54 \times 10^{-3} \text{ lb/ft}^{3/2}\text{-sec-atm}^{1/2} \text{ (data pt. Figure 34)}$$

Similarly,

$$\dot{m}\sqrt{\frac{R_B}{P_e}} = 5.22 \times 10^{-3} \left(\frac{6.41 \times 10^{-3}}{7.70 \times 10^{-3}}\right)^{1/2}$$

$$= 4.78 \times 10^{-3} \text{ lb/ft}^{3/2}\text{-sec-atm}^{1/2} \text{ (data pt. Figure 35)}$$

Thus, each datum point for comparison with the theory is established,

calculated in the form pertinent to the type presentation for which it is to be

used.

TABLE 1

SUMMARY OF TOTAL CALORIMETER

ENTHALPY MEASUREMENTS

| $E_k$, KW | $\dot{m}$, lb/sec. | $P_s$, psia | $h_s/RT_o$ | $h_s$, Btu/lb. |
|---|---|---|---|---|
| 238 | .0015 | 22.2 | 351 | 11880 |
| 238 | | 20.8 | 327 | 11070 |
| 230 | | 20.6 | 316 | 10700 |
| 283 | ↓ | 19.5 | 332 | 11230 |
| | | | | |
| 76.7 | .0014 | 16.0 | 157 | 5310 |
| 76.7 | | 15.9 | 166 | 5610 |
| 76.7 | | 16.0 | 162 | 5480 |
| 87.5 | ↓ | 16.3 | 162 | 5480 |

TABLE 2

SUMMARY OF COLD WALL HEAT TRANSFER MEASUREMENTS
FLAT FACE SPECIMENS

| Configuration [1] | Nozzle | Position [2] | Nominal $h_s/RT_o$ | Heat Transfer Rates |
|---|---|---|---|---|
| 1"D-1/4"d | 5.0" | 0.563" | 350 | 75.0 Btu/ft-sec$^2$ |
| | | 1.500 | | 76.0 |
| | | " | | 68.5 |
| | | 1.850 | | 76.0 |
| | | " | | 63.5 |
| | | " | | 58.5 |
| | | 2.225 | | 71.5 |
| | | " | | 69.5 |
| 1/4"D-1/8"d | | 0.563 | | 144.5 |
| | | 1.500 | | 139.0 |
| 1/4"d [3] | | 0.563 | | 141.0 |
| 1/4"D-1/8"d | 1.2 | 0.563 | | 130.0 |
| | | " | | 482 |
| | | " | | 497 |
| 1/4"d [3] | 5.0 | 1.500 | | 505 |
| 1/16"d [3] | | " | | 269 |
| | | " | | 283 |
| | | | | 288 |
| 1"D-1/4"d | 5.0 | 0.800 | 160 | 49.0 |
| | | " | | 48.6 |

[1] Configuration: Gives model dia. followed by copper insert dia.
[2] Station: Distance to stagnation point, from nozzle exit
[3] Copper cylinder with .003" RTV coating

## TABLE 3
### SUMMARY OF MASS RATE DATA

Specimen Dia.  1/4"  
Specimen Mat'l  ATJ  
Nozzle Exit Dia.  5"  
Stag'n Press., atm  $8.25 \times 10^{-3}$  
Enthalpy Ratio  350  
Reynolds No., $Re_s$  11  

Notes -
(1) Unmodified data
(2) Data modified for Reynolds No. Effects
☐ Symbol on graphs

| Run Nos. | Time Sec. | Mass Loss Lb/ft.$^2$ | Avg. °K Temp. | Mass Rate $\times 10^3$ lb/ft$^2$ - sec (1) | (2) | $\dot{m}\sqrt{\frac{Rb}{Pe}} \times 10^3$ lb/ft$^{3/2}$-sec-Atm$^{1/2}$ (1) | (2) |
|---|---|---|---|---|---|---|---|
| 472 | 80 | .1197 | | | | | |
| 463 | 39 | .0459 | | | | | |
| | 41 | .0738 | 1425 | 1.93 | 2.185 | 3.42 | 3.875 |
| 473 | 120 | .1980 | | | | | |
| 472 | 80 | .1197 | | | | | |
| | 40 | .0783 | 1485 | 1.995 | 2.065 | 3.53 | 3.83 |
| 462 | 127 | .2187 | | | | | |
| 472 | 80 | .1197 | | | | | |
| | 47 | .0990 | 1480 | 2.155 | 2.35 | 3.56 | 3.88 |
| 474 | 160 | .2898 | | | | | |
| 462 | 127 | .2187 | | | | | |
| | 33 | .0711 | 1405 | 2.195 | 2.52 | 3.57 | 4.13 |
| 474 | 160 | .2898 | | | | | |
| 473 | 120 | .1980 | | | | | |
| | 40 | .0918 | 1435 | 2.34 | 2.64 | 3.60 | 4.06 |
| 473 | 120 | .1980 | | | | | |
| 463 | 39 | .0459 | | | | | |
| | 81 | .1521 | 1400 | 1.915 | 2.225 | 3.39 | 3.93 |
| 458 | 128 | .1791 | | | | | |
| 461 | 100 | .1377 | | | | | |
| | 28 | .0414 | 1385 | 1.54 | 1.82 | 2.72 | 3.21 |
| 458 | 128 | .1791 | | | | | |
| 459 | 100 | .1089 | | | | | |
| | 28 | .0702 | 1370 | 2.56 | 3.06 | 4.53 | 5.42 |
| 474 | 160 | .2898 | | | | | |
| 461 | 100 | .1377 | | | | | |
| | 60 | .1521 | 1410 | 2.585 | 2.965 | 4.58 | 5.26 |
| 474 | 160 | .2898 | | | | | |
| 459 | 100 | .1089 | | | | | |
| | 60 | .1809 | 1400 | 3.075 | 3.57 | 5.44 | 6.30 |

TABLE 3
SUMMARY OF MASS RATE DATA

Specimen Dia.          1/4"                    Notes -
Specimen Mat'l         ATJ                       (1) Unmodified data
Nozzle Exit Dia.       5"                        (2) Data modified for
Stag'n Press., atm     $8.25 \times 10^{-3}$         Reynolds No. Effects
Enthalpy Ratio         350                       ▣  Symbol on graphs
Reynolds No., $Re_s$   11

| Run Nos. | Time Sec. | Mass Loss Lb/ft$^2$ | Avg. $^\circ$K Temp. | Mass Rate x 10$^3$ lb/ft$^2$ - sec (1) | (2) | $\dot{m}\sqrt{\dfrac{Rb}{Pe}} \times 10^3$ lb/ft$^{3/2}$-sec-Atm$^{1/2}$ (1) | (2) |
|---|---|---|---|---|---|---|---|
| 473 | 120 | .1980 | | | | | |
| 461 | 100 | .1377 | | | | | |
|     | 20  | .0603 | 1410 | 3.07 | 3.53 | 5.43 | 6.24 |
| 462 | 127 | .2187 | | | | | |
| 461 | 100 | .1377 | | | | | |
|     | 27  | .0810 | 1405 | 3.06 | 3.55 | 5.42 | 6.28 |
| 462 | 127 | .2187 | | | | | |
| 473 | 120 | .1980 | | | | | |
|     | 7   | .0207 | 1425 | 3.015 | 3.415 | 5.34 | 6.05 |
| 474 | 160 | .2898 | | | | | |
| 472 | 80  | .1197 | | | | | |
|     | 80  | .1701 | 1440 | 2.175 | 2.44 | 3.87 | 4.34 |
| 463 | 39  | .0459 | 1300 | 1.20 | 1.655 | 2.12 | 2.92 |
| 461 | 100 | .1377 | 1320 | 1.40 | 1.825 | 2.48 | 4.05 |
| 473 | 120 | .1980 | 1300 | 1.68 | 2.035 | 2.97 | 3.61 |
| 462 | 127 | .2187 | 1340 | 1.79 | 2.25 | 3.16 | 3.97 |
| 474 | 160 | .2898 | 1300 | 1.85 | 2.25 | 3.28 | 3.99 |

TABLE 4

SUMMARY OF MASS RATE DATA

| | | | |
|---|---|---|---|
| Specimen Dia. | 1/4" | Notes - | |
| Specimen Mat'l | ATJ | (1) | Unmodified data |
| Nozzle Exit Dia. | 1.2" | (2) | Data modified for |
| Stag'n Press., atm | $5.60 \times 10^{-2}$ | | Reynolds No. Effects |
| Enthalpy Ratio | 350 | ⊙ | Symbol on graphs |
| Reynolds No., $Re_s$ | 85 | | |

| Run Nos. | Time Sec. | Mass Loss Lb/ft.$^2$ | Avg. $^\circ K$ Temp. | Mass Rate $\times 10^3$ lb/ft$^2$ - sec (1) | (2) | $\dot{m}\sqrt{\dfrac{Rb}{Pe}} \times 10^3$ lb/ft$^{3/2}$-sec-Atm$^{1/2}$ (1) | (2) |
|---|---|---|---|---|---|---|---|
| 496 | 80 | .8415 | | | | | |
| 494 | 45 | .4392 | | | | | |
| | 35 | .4023 | 2150 | 11.50 | 8.86 | 7.80 | 6.07 |
| 501 | 87.5 | .9702 | | | | | |
| 494 | 45 | .4392 | | | | | |
| | 42.5 | .5310 | 2125 | 12.48 | 9.71 | 8.46 | 6.58 |
| 495 | 100 | 1.0404 | | | | | |
| 494 | 45 | .4392 | | | | | |
| | 55 | .6012 | 2175 | 11.14 | 8.68 | 7.56 | 5.88 |
| 489 | 100 | 1.0593 | | | | | |
| 494 | 45 | .4392 | | | | | |
| | 55 | .6201 | 2230 | 11.29 | 8.77 | 7.65 | 5.95 |
| 490 | 130 | 1.4103 | | | | | |
| 494 | 45 | .4392 | | | | | |
| | 85 | .9711 | 2660 | 11.42 | 8.84 | 7.75 | 6.00 |
| 498 | 130 | 1.4490 | | | | | |
| 494 | 45 | .4392 | | | | | |
| | 85 | 1.0108 | 2160 | 11.83 | 9.19 | 8.02 | 6.24 |
| 497 | 160 | 1.7460 | | | | | |
| 494 | 45 | .4392 | | | | | |
| | 115 | 1.3068 | 2160 | 11.34 | 8.81 | 7.69 | 5.98 |
| 488 | 165 | 1.9440 | | | | | |
| 494 | 45 | .4392 | | | | | |
| | 120 | 1.4048 | 2320 | 11.70 | 9.08 | 7.94 | 6.16 |
| 501 | 100 | 1.0602 | | | | | |
| 494 | 45 | .4392 | | | | | |
| | 55 | .6210 | 2180 | 11.28 | 8.77 | 7.65 | 5.95 |

## TABLE 4
### SUMMARY OF MASS RATE DATA

| Specimen Dia. | 1/4" | Notes – |
|---|---|---|
| Specimen Mat'l | ATJ | (1) Unmodified data |
| Nozzle Exit Dia. | 1.2" | (2) Data modified for |
| Stag'n Press., atm | $5.60 \times 10^{-2}$ | Reynolds No. Effects |
| Enthalpy Ratio | 350 | ⊙ Symbol on graphs |
| Reynolds No., $Re_s$ | 85 | |

| Run Nos. | Time Sec. | Mass Loss Lb/ft.$^2$ | Avg. °K Temp. | Mass Rate $\times 10^3$ lb/ft$^2$ – sec (1) | (2) | $\dot{m}\sqrt{\dfrac{Rb}{Pe}} \times 10^3$ lb/ft$^{3/2}$-sec-Atm$^{1/2}$ (1) | (2) |
|---|---|---|---|---|---|---|---|
| 489 | 100 | 1.0593 | | | | | |
| 496 | 80 | .8415 | | | | | |
| | 20 | .2178 | 2230 | 11.88 | 9.24 | 8.05 | 6.25 |
| 501 | 100 | 1.0602 | | | | | |
| 496 | 80 | .8415 | | | | | |
| | 20 | .2187 | 2180 | 11.90 | 9.25 | 8.07 | 6.28 |
| 498 | 130 | 1.4490 | | | | | |
| 496 | 80 | .8415 | | | | | |
| | 50 | .6075 | 2160 | 12.14 | 9.44 | 8.23 | 6.39 |
| 490 | 130 | 1.4103 | | | | | |
| 496 | 80 | .8415 | | | | | |
| | 50 | .5688 | 2660 | 11.37 | 8.80 | 7.71 | 5.97 |
| 497 | 160 | 1.7460 | | | | | |
| 496 | 80 | .8415 | | | | | |
| | 80 | .9045 | 2160 | 11.30 | 8.79 | 7.66 | 5.95 |
| 488 | 165 | 1.9440 | | | | | |
| 496 | 80 | .8415 | | | | | |
| | 85 | 1.1025 | 2320 | 12.95 | 10.08 | 8.78 | 6.72 |
| 498 | 130 | 1.4490 | | | | | |
| 501 | 87.5 | .9702 | | | | | |
| | 42.5 | .4788 | 2135 | 11.28 | 8.77 | 7.65 | 5.95 |
| 488 | 165 | 1.9440 | | | | | |
| 501 | 87.5 | .9702 | | | | | |
| | 77.5 | .9738 | 2290 | 12.57 | 9.76 | 8.52 | 6.62 |
| 490 | 130 | 1.4103 | | | | | |
| 495 | 100 | 1.0404 | | | | | |
| | 30 | .3699 | 2685 | 12.32 | 9.55 | 8.35 | 6.45 |

TABLE 4

SUMMARY OF MASS RATE DATA

| | | Notes - |
|---|---|---|
| Specimen Dia. | 1/4" | (1) Unmodified data |
| Specimen Mat'l | ATJ | (2) Data modified for |
| Nozzle Exit Dia. | 1.2" | Reynolds No. Effects |
| Stag'n Press., atm | $5.60 \times 10^{-2}$ | ⊙ Symbol on graphs |
| Enthalpy Ratio | 350 | |
| Reynolds No., $Re_s$ | 85 | |

| Run Nos. | Time Sec. | Mass Loss $Lb/ft^2$ | Avg. °K Temp. | Mass Rate $\times 10^3$ $lb/ft^2$ - sec | | $\dot{m}\sqrt{\frac{Rb}{Pe}} \times 10^3$ $lb/ft^{3/2}$-sec-$Atm^{1/2}$ | |
|---|---|---|---|---|---|---|---|
| | | | | (1) | (2) | (1) | (2) |
| 497 | 160 | 1.7460 | | | | | |
| 495 | 100 | 1.0404 | | | | | |
| | 60 | .7056 | 2185 | 11.77 | 9.14 | 7.98 | 6.20 |
| 488 | 165 | 1.9440 | 2350 | 11.77 | 9.11 | 7.98 | 6.11 |
| 498 | 130 | 1.4490 | 2170 | 11.13 | 8.66 | 7.55 | 5.87 |
| 501 | 87.5 | .9702 | 2100 | 11.08 | 8.62 | 7.51 | 5.85 |
| 490 | 130 | 1.4103 | | | | | |
| 489 | 100 | 1.0593 | | | | | |
| | 30 | .3510 | 2740 | 11.70 | 9.06 | 7.94 | 6.17 |
| 497 | 160 | 1.7640 | | | | | |
| 489 | 100 | 1.0593 | | | | | |
| | 60 | .7047 | 2280 | 11.77 | 9.15 | 7.98 | 6.20 |
| 490 | 130 | 1.4103 | | | | | |
| 501 | 100 | 1.0602 | | | | | |
| | 30 | .3501 | 2690 | 11.69 | 9.05 | 7.92 | 6.06 |
| 497 | 160 | 1.7640 | | | | | |
| 501 | 100 | 1.0602 | | | | | |
| | 60 | .7038 | 2190 | 11.72 | 9.13 | 7.95 | 6.11 |
| 497 | 160 | 1.7640 | | | | | |
| 490 | 130 | 1.4103 | | | | | |
| | 30 | .3537 | 2670 | 11.76 | 9.10 | 7.98 | 6.18 |

### TABLE 5
#### SUMMARY OF MASS RATE DATA

Specimen Dia.    1"       Notes -
Specimen Mat'l    ATJ      (1) Unmodified data
Nozzle Exit Dia.    5"      (2) Data modified for
Stag'n Press., atm    $9.7 \times 10^{-3}$      Reynolds No. Effects
Enthalpy Ratio    400      $\triangle$   Symbol on graphs
Reynolds No., $Re_s$    44

| Run Nos. | Time Sec. | Mass Loss $Lb/ft^2$ | Avg. °K Temp. | Mass Rate $\times 10^3$ $lb/ft^2$ - sec (1) | (2) | $\dot{m}\sqrt{\dfrac{Rb}{Pe}} \times 10^3$ $lb/ft^{3/2}$-sec-$Atm^{1/2}$ (1) | (2) |
|---|---|---|---|---|---|---|---|
| 303 | 120 | .0936 | | | | | |
| 305 | 60 | .0324 | | | | | |
|  | 60 | .0612 | 1235 | 1.019 | 1.112 | 3.31 | 3.61 |
| 308 | 150 | .1224 | | | | | |
| 305 | 60 | .0324 | | | | | |
|  | 90 | .0900 | 1245 | 1.00 | 1.080 | 3.25 | 3.51 |
| 311 | 180 | .1467 | | | | | |
| 305 | 60 | .0324 | | | | | |
|  | 120 | .1143 | 1245 | .939 | 1.013 | 3.05 | 3.19 |
| 316 | 240 | .2007 | | | | | |
| 305 | 60 | .0324 | | | | | |
|  | 180 | .1683 | 1245 | .897 | .969 | 2.92 | 3.15 |
| 307 | 110 | .0828 | | | | | |
| 306 | 100 | .0711 | | | | | |
|  | 10 | .0117 | 1280 | 1.171 | 1.211 | 3.81 | 3.94 |
| 303 | 120 | .0936 | | | | | |
| 306 | 100 | .0711 | | | | | |
|  | 20 | .0225 | 1290 | 1.127 | 1.139 | 3.68 | 3.72 |
| 308 | 150 | .1224 | | | | | |
| 306 | 100 | .0711 | | | | | |
|  | 50 | .0513 | 1300 | 1.023 | 1.021 | 3.33 | 3.32 |
| 311 | 180 | .1467 | | | | | |
| 306 | 100 | .0711 | | | | | |
|  | 80 | .0756 | 1300 | .947 | .945 | 3.08 | 3.07 |
| 316 | 240 | .2007 | | | | | |
| 306 | 100 | .0711 | | | | | |
|  | 140 | .1296 | 1300 | .926 | .925 | 3.01 | 3.00 |
| 303 | 120 | .0936 | | | | | |
| 307 | 110 | .0828 | | | | | |
|  | 10 | .0108 | 1300 | 1.082 | 1.080 | 3.52 | 3.51 |

## TABLE 5
### SUMMARY OF MASS RATE DATA

Specimen Dia.          1"
Specimen Mat'l         ATJ
Nozzle Exit Dia.       5"
Stag'n Press., atm     $9.7 \times 10^{-3}$
Enthalpy Ratio         400
Reynolds No., $Re_s$   44

Notes -
(1) Unmodified data
(2) Data modified for Reynolds No. Effects
△ Symbol on graphs

| Run Nos. | Time Sec. | Mass Loss Lb/ft.$^2$ | Avg. $^\circ$K Temp. | Mass Rate $\times 10^3$ lb/ft$^2$ - sec (1) | (2) | $\dot{m}\sqrt{\dfrac{Rb}{Pe}} \times 10^3$ /ft$^{3/2}$-sec-Atm$^{1/2}$ (1) | (2) |
|---|---|---|---|---|---|---|---|
| 308 | 150 | .1224 | | | | | |
| 307 | 110 | .0828 | | | | | |
|     | 40  | .0396 | 1310 | .988 | .968 | 3.21 | 3.16 |
| 311 | 180 | .1467 | | | | | |
| 307 | 110 | .0828 | | | | | |
|     | 70  | .0639 | 1310 | .909 | .892 | 2.96 | 2.91 |
| 316 | 240 | .2007 | | | | | |
| 307 | 110 | .0828 | | | | | |
|     | 130 | .1179 | 1310 | .906 | .890 | 2.94 | 2.89 |
| 308 | 150 | .1224 | | | | | |
| 303 | 120 | .0936 | | | | | |
|     | 30  | .0288 | 1320 | .964 | .930 | 3.13 | 3.02 |
| 311 | 180 | .1467 | | | | | |
| 303 | 120 | .0936 | | | | | |
|     | 60  | .0531 | 1320 | .885 | .854 | 2.88 | 2.78 |
| 316 | 240 | .2007 | | | | | |
| 303 | 120 | .0936 | | | | | |
|     | 120 | .1071 | 1320 | .890 | .859 | 2.90 | 2.80 |
| 311 | 180 | .1467 | | | | | |
| 308 | 150 | .1224 | | | | | |
|     | 30  | .0243 | 1330 | .811 | .770 | 2.64 | 2.505 |
| 316 | 240 | .2007 | | | | | |
| 308 | 150 | .1224 | | | | | |
|     | 90  | .0783 | 1330 | .868 | .823 | 2.82 | 2.68 |
| 316 | 240 | .2007 | | | | | |
| 311 | 180 | .1467 | | | | | |
|     | 60  | .0540 | 1330 | .902 | .856 | 2.93 | 2.78 |

## TABLE 5
### SUMMARY OF MASS RATE DATA

Specimen Dia.  1"  
Specimen Mat'l  ATJ  
Nozzle Exit Dia.  5"  
Stag'n Press., atm  $9.7 \times 10^{-3}$  
Enthalpy Ratio  400  
Reynolds No., $Re_s$  44  

Notes -  
(1) Unmodified data  
(2) Data modified for Reynolds No. Effects  
△ Symbol on graphs

| Run Nos. | Time Sec. | Mass Loss Lb/ft.$^2$ | Avg. $^\circ$K Temp. | Mass Rate $\times 10^3$ lb/ft$^2$ - sec (1) | (2) | $\dot{m}\sqrt{\frac{Rb}{Pe}} \times 10^3$ lb/ft$^{3/2}$-sec-Atm$^{1/2}$ (1) | (2) |
|---|---|---|---|---|---|---|---|
| 327 | 300 | .720 | | | | | |
| 323 | 63 | .126 | | | | | |
| | 237 | .594 | 1670 | 2.50 | 2.075 | 8.12 | 6.23 |
| 326 | 240 | .567 | | | | | |
| 323 | 63 | .126 | | | | | |
| | 177 | .441 | 1685 | 2.49 | 2.065 | 8.10 | 6.21 |
| 322 | 213 | .495 | | | | | |
| 323 | 63 | .126 | | | | | |
| | 150 | .369 | 1745 | 2.46 | 2.03 | 8.00 | 6.10 |
| 325 | 139 | .297 | | | | | |
| 323 | 63 | .126 | | | | | |
| | 76 | .171 | 1685 | 2.31 | 1.908 | 7.52 | 5.74 |
| 327 | 300 | .720 | | | | | |
| 324 | 77 | .153 | | | | | |
| | 223 | .567 | 1680 | 2.54 | 2.108 | 8.25 | 6.32 |
| 326 | 240 | .567 | | | | | |
| 324 | 77 | .153 | | | | | |
| | 163 | .414 | 1695 | 2.54 | 2.108 | 8.25 | 6.32 |
| 322 | 213 | .495 | | | | | |
| 324 | 77 | .153 | | | | | |
| | 136 | .342 | 1755 | 2.52 | 2.075 | 8.19 | 6.24 |
| 325 | 139 | .297 | | | | | |
| 324 | 77 | .153 | | | | | |
| | 62 | .144 | 1695 | 2.33 | 1.934 | 7.58 | 5.82 |
| 327 | 300 | .720 | | | | | |
| 325 | 139 | .297 | | | | | |
| | 161 | .423 | 1690 | 2.63 | 2.18 | 8.55 | 6.55 |

TABLE 5

SUMMARY OF MASS RATE DATA

| | | |
|---|---|---|
| Specimen Dia. | 1" | **Notes -** |
| Specimen Mat'l | ATJ | (1) Unmodified data |
| Nozzle Exit Dia. | 5" | (2) Data modified for |
| Stag'n Press., atm | $9.7 \times 10^{-3}$ | Reynolds No. Effects |
| Enthalpy Ratio | 400 | $\triangle$ Symbol on graphs |
| Reynolds No., $Re_s$ | 44 | |

| Run Nos. | Time Sec. | Mass Loss Lb/ft.$^2$ | Avg. $^\circ$K Temp. | Mass Rate $\times 10^3$ lb/ft$^2$ - sec (1) | Mass Rate $\times 10^3$ lb/ft$^2$ - sec (2) | $\dot{m}\sqrt{\dfrac{Rb}{Pe}} \times 10^3$ lb/ft$^{3/2}$-sec-Atm$^{1/2}$ (1) | $\dot{m}\sqrt{\dfrac{Rb}{Pe}} \times 10^3$ lb/ft$^{3/2}$-sec-Atm$^{1/2}$ (2) |
|---|---|---|---|---|---|---|---|
| 326 | 240 | .567 | | | | | |
| 325 | 139 | .297 | | | | | |
| | 101 | .270 | 1710 | 2.67 | 2.21 | 8.68 | 6.63 |
| 322 | 213 | .495 | | | | | |
| 325 | 139 | .297 | | | | | |
| | 74 | .198 | 1770 | 2.68 | 2.21 | 8.71 | 6.64 |
| 327 | 300 | .720 | | | | | |
| 322 | 213 | .495 | | | | | |
| | 87 | .225 | 1750 | 2.59 | 2.138 | 8.42 | 6.43 |
| 326 | 240 | .567 | | | | | |
| 322 | 213 | .495 | | | | | |
| | 27 | .072 | 1770 | 2.67 | 2.20 | 8.68 | 6.61 |
| 327 | 300 | .720 | | | | | |
| 326 | 240 | .567 | | | | | |
| | 60 | .153 | 1690 | 2.55 | 2.115 | 8.29 | 6.35 |
| 323 | 63 | .126 | 1350 | 2.00 | 1.833 | 6.50 | 6.02 |
| 324 | 77 | .153 | 1450 | 1.99 | 1.73 | 6.47 | 5.63 |
| 325 | 139 | .297 | 1450 | 2.14 | 1.86 | 6.95 | 6.04 |
| 322 | 213 | .495 | 1750 | 2.32 | 1.915 | 7.54 | 5.75 |
| 326 | 240 | .567 | 1630 | 2.37 | 1.975 | 7.70 | 5.93 |
| 327 | 300 | .720 | 1600 | 2.40 | 2.008 | 7.80 | 6.03 |

TABLE 6

SUMMARY OF MASS RATE DATA

| | | | Notes - | | |
|---|---|---|---|---|---|
| Specimen Dia. | 1" | | (1) Unmodified data | | |
| Specimen Mat'l | ATJ | | (2) Data modified for | | |
| Nozzle Exit Dia. | 1.2" | | Reynolds No. Effects | | |
| Stag'n Press., atm | $4.43 \times 10^{-2}$ | | ◇ Symbol on graphs | | |
| Enthalpy Ratio | 400 | | | | |
| Reynolds No., $Re_s$ | 342 | | | | |

| Run Nos. | Time Sec. | Mass Loss Lb/ft.$^2$ | Avg. $^\circ$K Temp. | Mass Rate $\times 10^3$ lb/ft$^2$ - sec (1) | (2) | $\dot{m}\sqrt{\dfrac{Rb}{Pe}} \times 10^3$ lb/ft$^{3/2}$-sec-Atm$^{1/2}$ (1) | (2) |
|---|---|---|---|---|---|---|---|
| 342 | 200 | 1.0017 | | | | | |
| 330 | 39 | .216 | | | | | |
| | 161 | 0.7857 | 2050 | 4.88 | 3.71 | 7.46 | 5.68 |
| | | | | | | | |
| 331 | 100 | .513 | | | | | |
| 330 | 39 | .216 | | | | | |
| | 61 | .297 | 1825 | 4.88 | 3.74 | 7.46 | 5.73 |
| | | | | | | | |
| 342 | 200 | 1.0017 | | | | | |
| 336 | 60 | .2970 | | | | | |
| | 140 | .7047 | 1790 | 5.05 | 3.88 | 7.71 | 5.92 |
| | | | | | | | |
| 331 | 100 | .513 | | | | | |
| 336 | 60 | .297 | | | | | |
| | 40 | .216 | 1960 | 5.39 | 4.10 | 8.24 | 6.28 |
| | | | | | | | |
| 342 | 200 | 1.0017 | | | | | |
| 331 | 100 | .513 | | | | | |
| | 100 | .4887 | 2115 | 4.86 | 3.69 | 7.42 | 5.65 |
| | | | | | | | |
| 342 | 200 | 1.0017 | | | | | |
| 332 | 150 | .729 | | | | | |
| | 50 | .2727 | 2135 | 5.45 | 4.14 | 8.33 | 6.30 |
| | | | | | | | |
| 342 | 200 | 1.0017 | 1600 | 5.01 | 3.93 | 7.66 | 6.00 |
| | | | | | | | |
| 331 | 100 | .513 | 2050 | 5.12 | 3.89 | 7.83 | 5.95 |
| | | | | | | | |
| 330 | 39 | .216 | 1600 | 5.53 | 4.32 | 8.45 | 6.13 |

TABLE 7

SUMMARY OF MASS RATE DATA

Specimen Dia.          1/16"                          Notes -
Specimen Mat'l         ATJ                            (1) Unmodified data
Nozzle Exit Dia.       5"                             (2) Data modified for
Stag'n Press., atm     $7.70 \times 10^{-3}$               Reynolds No. Effects
Enthalpy Ratio         350
Reynolds No., $Re_B$   2.7                            ◐  Symbol on graphs

| Run Nos. | Time Sec. | Mass Loss Lb/ft$^2$ | Avg. °K Temp. | Mass Rate $\times 10^3$ lb/ft$^2$ - sec (1) | (2) | $\dot{m}\sqrt{\dfrac{Rb}{Pe}} \times 10^3$ lb/ft$^{3/2}$-sec-Atm$^{1/2}$ (1) | (2) |
|---|---|---|---|---|---|---|---|
| 560 | 250 | .6751 | | | | | |
| 521 | 60 | .1494 | | | | | |
|     | 190 | .5257 | 1515 | 2.77 | 5.21 | 2.54 | 4.78 |
| 560 | 250 | .6751 | | | | | |
| 520 | 120 | .3168 | | | | | |
|     | 130 | .3583 | 1520 | 2.75 | 5.15 | 2.52 | 4.73 |
| 560 | 250 | .6751 | | | | | |
| 519 | 120 | .2988 | | | | | |
|     | 130 | .3763 | 1540 | 2.90 | 5.38 | 2.66 | 4.94 |
| 560 | 250 | .6751 | | | | | |
| 518 | 100 | .2556 | | | | | |
|     | 150 | .4195 | 1545 | 2.80 | 5.17 | 2.56 | 4.73 |
| 560 | 250 | .6751 | | | | | |
| 517 | 100 | .2520 | | | | | |
|     | 150 | .4231 | 1560 | 2.82 | 5.15 | 2.58 | 4.72 |
| 560 | 250 | .6751 | | | | | |
| 516 | 80 | .1863 | | | | | |
|     | 170 | .4888 | 1545 | 2.87 | 5.30 | 2.62 | 4.84 |
| 560 | 250 | .6751 | | | | | |
| 515 | 80 | .2007 | | | | | |
|     | 170 | .4744 | 1520 | 2.79 | 5.23 | 2.55 | 4.79 |
| 560 | 250 | .6751 | | | | | |
| 514 | 60 | .1620 | | | | | |
|     | 190 | .5131 | 1500 | 2.70 | 5.13 | 2.47 | 4.70 |
| 560 | 250 | .6751 | | | | | |
| 513 | 40 | .1107 | | | | | |
|     | 210 | .5644 | 1485 | 2.69 | 5.17 | 2.46 | 4.72 |

## TABLE 7
### SUMMARY OF MASS RATE DATA

Specimen Dia.    1/16"            Notes –
Specimen Mat'l   ATJ           (1)  Unmodified data
Nozzle Exit Dia.   5"            (2)  Data modified for
Stag'n Press., atm  $7.70 \times 10^{-3}$         Reynolds No. Effects
Enthalpy Ratio    350        ⊕  Symbol on graphs
Reynolds No., $\bar{Re}_s$   2.7

| Run Nos. | Time Sec. | Mass Loss Lb/ft² | Avg. °K Temp. | Mass Rate $\times 10^3$ lb/ft²-sec (1) | (2) | $\dot{m}\sqrt{\dfrac{Rb}{Pe}} \times 10^3$ lb/ft$^{3/2}$-sec-Atm$^{1/2}$ (1) | (2) |
|---|---|---|---|---|---|---|---|
| 558 | 200 | .5454 | | | | | |
| 557 | 100 | .2205 | | | | | |
| | 100 | .3249 | 1615 | 2.35 | 5.75 | 2.97 | 4.79 |
| 558 | 200 | .5454 | | | | | |
| 521 | 60 | .1494 | | | | | |
| | 140 | .3960 | 1525 | 2.83 | 5.29 | 2.59 | 4.85 |
| 558 | 200 | .5454 | | | | | |
| 520 | 120 | .3168 | | | | | |
| | 80 | .2286 | 1530 | 2.86 | 5.33 | 2.62 | 4.89 |
| 558 | 200 | .5454 | | | | | |
| 519 | 120 | .2988 | | | | | |
| | 80 | .2466 | 1550 | 3.08 | 5.65 | 2.82 | 4.99 |
| 558 | 200 | .5454 | | | | | |
| 518 | 100 | .2556 | | | | | |
| | 100 | .2898 | 1555 | 2.90 | 5.31 | 2.65 | 4.85 |
| 558 | 200 | .5454 | | | | | |
| 517 | 100 | .2520 | | | | | |
| | 100 | .2934 | 1570 | 2.93 | 5.31 | 2.68 | 4.86 |
| 558 | 200 | .5454 | | | | | |
| 516 | 80 | .1863 | | | | | |
| | 120 | .3591 | 1555 | 2.99 | 5.47 | 2.74 | 5.02 |
| 558 | 200 | .5454 | | | | | |
| 515 | 80 | .2007 | | | | | |
| | 120 | .3447 | 1530 | 2.87 | 5.34 | 2.63 | 4.90 |
| 558 | 200 | .5454 | | | | | |
| 514 | 60 | .1620 | | | | | |
| | 140 | .3834 | 1510 | 2.74 | 5.17 | 2.51 | 4.74 |

**TABLE 7**

SUMMARY OF MASS RATE DATA

| | | |
|---|---|---|
| Specimen Dia. | 1/16" | Notes - |
| Specimen Mat'l | ATJ | (1) Unmodified data |
| Nozzle Exit Dia. | 5" | (2) Data modified for |
| Stag'n Press., atm | $7.70 \times 10^{-3}$ | Reynolds No. Effects |
| Enthalpy Ratio | 350 | ● Symbol on graphs |
| Reynolds No., $Re_s$ | 2.7 | |

| Run Nos. | Time Sec. | Mass Loss Lb/ft.$^2$ | Avg. $^\circ$K Temp. | Mass Rate $\times 10^3$ lb/ft$^2$ - sec (1) | (2) | $\dot{m}\sqrt{\frac{Rb}{Pe}} \times 10^3$ lb/ft$^{3/2}$-sec-Atm$^{1/2}$ (1) | (2) |
|---|---|---|---|---|---|---|---|
| 558 | 200 | .5454 | | | | | |
| 513 | 40 | .1107 | | | | | |
| | 160 | .4347 | 1495 | 2.72 | 5.20 | 2.49 | 4.75 |
| 559 | 150 | .3954 | | | | | |
| 557 | 100 | .2205 | | | | | |
| | 50 | .1749 | 1640 | 3.49 | 6.22 | 3.19 | 5.69 |
| 559 | 150 | .3954 | | | | | |
| 521 | 60 | .1494 | | | | | |
| | 90 | .2460 | 1550 | 2.73 | 5.02 | 2.50 | 4.60 |
| 559 | 150 | .3954 | | | | | |
| 520 | 120 | .3168 | | | | | |
| | 30 | .0786 | 1555 | 2.62 | 4.79 | 2.40 | 4.40 |
| 559 | 150 | .3954 | | | | | |
| 519 | 120 | .2988 | | | | | |
| | 30 | .0966 | 1575 | 3.22 | 5.85 | 2.95 | 5.35 |
| 559 | 150 | .3954 | | | | | |
| 518 | 100 | .2556 | | | | | |
| | 50 | .1398 | 1580 | 2.79 | 5.05 | 2.55 | 4.62 |
| 559 | 150 | .3954 | | | | | |
| 517 | 100 | .2520 | | | | | |
| | 50 | .1434 | 1595 | 2.87 | 5.15 | 2.63 | 4.72 |
| 559 | 150 | .3954 | | | | | |
| 516 | 80 | .1863 | | | | | |
| | 70 | .2091 | 1580 | 2.98 | 5.40 | 2.72 | 4.92 |
| 559 | 150 | .3954 | | | | | |
| 515 | 80 | .2007 | | | | | |
| | 70 | .1947 | 1555 | 2.78 | 5.09 | 2.54 | 4.65 |
| 559 | 150 | .3754 | | | | | |
| 514 | 60 | .1620 | | | | | |
| | 90 | .2334 | 1535 | 2.54 | 4.65 | 2.32 | 4.25 |

TABLE 7
SUMMARY OF MASS RATE DATA

| | | | Notes - |
|---|---|---|---|
| Specimen Dia. | 1/16" | | (1) Unmodified data |
| Specimen Mat'l | ATJ | | (2) Data modified for |
| Nozzle Exit Dia. | 5" | | Reynolds No. Effects |
| Stag'n Press., atm | $7.70 \times 10^{-3}$ | | ⊙ Symbol on graphs |
| Enthalpy Ratio | 350 | | |
| Reynolds No., $Re_s$ | 2.7 | | |

| Run Nos. | Time Sec. | Mass Loss Lb/ft.$^2$ | Avg. $^{\circ}$K Temp. | Mass Rate $\times 10^3$ lb/ft$^2$ - sec (1) | (2) | $\dot{m}\sqrt{\dfrac{Rb}{Pe}} \times 10^3$ lb/ft$^{3/2}$-sec-Atm$^{1/2}$ (1) | (2) |
|---|---|---|---|---|---|---|---|
| 559 | 150 | .3954 | | | | | |
| 513 | 40 | .1107 | | | | | |
| | 110 | .2847 | 1520 | 2.59 | 4.85 | 2.37 | 4.44 |
| 557 | 100 | .2205 | | | | | |
| 513 | 40 | .1107 | | | | | |
| | 60 | .1098 | 1480 | 1.83 | 3.53 | 1.68 | 3.24 |
| 521 | 60 | .1495 | | | | | |
| 513 | 40 | .1107 | | | | | |
| | 20 | .0588 | 1445 | 2.99 | 5.90 | 2.74 | 5.41 |
| 520 | 120 | .3168 | | | | | |
| 521 | 60 | .1494 | | | | | |
| | 60 | .1674 | 1465 | 2.78 | 5.43 | 2.54 | 4.95 |
| 520 | 120 | .3168 | | | | | |
| 518 | 100 | .2556 | | | | | |
| | 20 | .0612 | 1495 | 3.06 | 5.83 | 2.80 | 5.33 |
| 520 | 120 | .3168 | | | | | |
| 517 | 100 | .2520 | | | | | |
| | 20 | .0648 | 1510 | 3.24 | 6.12 | 2.96 | 5.59 |
| 520 | 120 | .3168 | | | | | |
| 516 | 80 | .1863 | | | | | |
| | 40 | .1305 | 1495 | 3.26 | 6.22 | 2.98 | 5.69 |
| 520 | 120 | .3168 | | | | | |
| 515 | 80 | .2007 | | | | | |
| | 40 | .1161 | 1470 | 2.91 | 5.65 | 2.66 | 5.17 |
| 520 | 120 | .3168 | | | | | |
| 514 | 60 | .1620 | | | | | |
| | 60 | .1548 | 1450 | 2.58 | 5.08 | 2.36 | 4.65 |

TABLE 7
SUMMARY OF MASS RATE DATA

Specimen Dia.        1/16"                    Notes -
Specimen Mat'l       ATJ                        (1) Unmodified data
Nozzle Exit Dia.     5"                         (2) Data modified for
Stag'n Press., atm   $7.70 \times 10^{-3}$          Reynolds No. Effects
Enthalpy Ratio       350                        ◉ Symbol on graphs
Reynolds No., $Re_s$  2.7

| Run Nos. | Time Sec. | Mass Loss Lb/ft.$^2$ | Avg. $^{\circ}$K Temp. | Mass Rate $\times 10^3$ lb/ft$^2$ - sec (1) | (2) | $\dot{m}\sqrt{\dfrac{Rb}{Pe}} \times 10^3$ lb/ft$^{3/2}$-sec-Atm$^{1/2}$ (1) | (2) |
|---|---|---|---|---|---|---|---|
| 520 | 120 | .3168 | | | | | |
| 513 | 40 | .1107 | | | | | |
| | 80 | .2061 | 1435 | 2.57 | 5.11 | 2.35 | 4.64 |
| 519 | 120 | .2988 | | | | | |
| 521 | 60 | .1494 | | | | | |
| | 60 | .1494 | 1480 | 2.49 | 4.80 | 2.28 | 4.40 |
| 519 | 120 | .2988 | | | | | |
| 518 | 100 | .2556 | | | | | |
| | 20 | .0432 | 1510 | 2.15 | 4.00 | 1.97 | 3.67 |
| 519 | 120 | .2988 | | | | | |
| 517 | 100 | .2520 | | | | | |
| | 20 | .0468 | 1475 | 2.34 | 4.54 | 2.14 | 4.15 |
| 519 | 120 | .2988 | | | | | |
| 516 | 80 | .1863 | | | | | |
| | 40 | .1125 | 1510 | 2.81 | 5.23 | 2.57 | 4.79 |
| 519 | 120 | .2988 | | | | | |
| 515 | 80 | .2007 | | | | | |
| | 40 | .0979 | 1485 | 2.45 | 4.70 | 2.24 | 4.30 |
| 519 | 120 | .2988 | | | | | |
| 514 | 60 | .1620 | | | | | |
| | 60 | .1368 | 1465 | 2.28 | 4.45 | 2.08 | 4.06 |
| 519 | 120 | .2988 | | | | | |
| 513 | 40 | .1107 | | | | | |
| | 80 | .1881 | 1450 | 2.35 | 4.61 | 2.15 | 4.22 |
| 518 | 100 | .2556 | | | | | |
| 521 | 60 | .1494 | | | | | |
| | 40 | .1062 | 1475 | 2.66 | 5.15 | 2.43 | 4.70 |

### TABLE 7
#### SUMMARY OF MASS RATE DATA

Specimen Dia.    1/16"  
Specimen Mat'l    ATJ  
Nozzle Exit Dia.    5"  
Stag'n Press., atm    $7.70 \times 10^{-3}$  
Enthalpy Ratio    350  
Reynolds No., $Re_s$    2.7  

Notes –  
(1) Unmodified data  
(2) Data modified for Reynolds No. Effects  
●   Symbol on graphs

| Run Nos. | Time Sec. | Mass Loss Lb/ft.$^2$ | Avg. °K Temp. | Mass Rate $\times 10^3$ lb/ft$^2$ – sec (1) | (2) | $\dot{m}\sqrt{\dfrac{Rb}{Pe}} \times 10^3$ lb/ft$^{3/2}$-sec-Atm$^{1/2}$ (1) | (2) |
|---|---|---|---|---|---|---|---|
| 518 | 100 | .2556 | | | | | |
| 516 | 80 | .1863 | | | | | |
| | 20 | .0693 | 1505 | 3.46 | 6.55 | 3.16 | 5.99 |
| 518 | 100 | .2556 | | | | | |
| 515 | 80 | .2007 | | | | | |
| | 20 | .0549 | 1480 | 2.74 | 5.20 | 2.51 | 4.84 |
| 518 | 100 | .2556 | | | | | |
| 514 | 60 | .1620 | | | | | |
| | 40 | .0936 | 1460 | 2.34 | 4.58 | 2.14 | 4.17 |
| 518 | 100 | .2556 | | | | | |
| 513 | 40 | .1107 | | | | | |
| | 60 | .1449 | 1445 | 2.41 | 4.75 | 2.21 | 4.36 |
| 517 | 100 | .2520 | | | | | |
| 521 | 60 | .1494 | | | | | |
| | 40 | .1026 | 1495 | 2.56 | 4.89 | 2.34 | 4.47 |
| 517 | 100 | .2520 | | | | | |
| 516 | 80 | .1494 | | | | | |
| | 20 | .0657 | 1525 | 3.29 | 6.15 | 3.01 | 5.63 |
| 517 | 100 | .2520 | | | | | |
| 515 | 80 | .2007 | | | | | |
| | 20 | .0513 | 1500 | 2.56 | 4.85 | 2.34 | 4.45 |
| 517 | 100 | .2520 | | | | | |
| 514 | 60 | .1620 | | | | | |
| | 40 | .0900 | 1480 | 2.24 | 4.26 | 2.05 | 3.95 |
| 517 | 100 | .2520 | | | | | |
| 513 | 40 | .1107 | | | | | |
| | 60 | .1413 | 1465 | 2.35 | 4.59 | 2.15 | 4.19 |

TABLE 7

SUMMARY OF MASS RATE DATA

Specimen Dia.        1/16"                      Notes -
Specimen Mat'l       ATJ                          (1) Unmodified data
Nozzle Exit Dia.     5"                           (2) Data modified for
Stag'n Press., atm   $7.70 \times 10^{-3}$            Reynolds No. Effects
Enthalpy Ratio       350                          ● Symbol on graphs
 Reynolds No., $Re_s$   2:7

| Run Nos. | Time Sec. | Mass Loss Lb/ft.$^2$ | Avg. $^\circ$K Temp. | Mass Rate $\times 10^3$ lb/ft$^2$ - sec | | $\dot{m}\sqrt{\dfrac{Rb}{Pe}} \times 10^3$ lb/ft$^{3/2}$-sec-Atm$^{1/2}$ | |
|---|---|---|---|---|---|---|---|
| | | | | (1) | (2) | (1) | (2) |
| 516 | 80 | .1863 | | | | | |
| 521 | 60 | .1494 | | | | | |
| | 20 | .0369 | 1470 | 1.85 | 3.60 | 1.69 | 3.28 |
| 516 | 80 | .1863 | | | | | |
| 513 | 40 | .1107 | | | | | |
| | 40 | .0756 | 1440 | 1.89 | 3.74 | 1.73 | 3.43 |
| 515 | 80 | .2007 | | | | | |
| 521 | 60 | .1494 | | | | | |
| | 20 | .0513 | 1475 | 2.56 | 5.00 | 2.34 | 4.53 |
| 515 | 80 | .2007 | | | | | |
| 514 | 60 | .1620 | | | | | |
| | 20 | .0387 | 1460 | 1.93 | 3.77 | 1.77 | 3.46 |
| 515 | 80 | .2007 | | | | | |
| 513 | 40 | .1107 | | | | | |
| | 40 | .0900 | 1445 | 2.24 | 4.42 | 2.05 | 4.04 |
| 521 | 60 | .1494 | | | | | |
| 513 | 40 | .1107 | | | | | |
| | 20 | .0387 | 1445 | 1.94 | 3.82 | 1.78 | 3.51 |
| 514 | 60 | .1620 | | | | | |
| 513 | 40 | .1107 | | | | | |
| | 20 | .0513 | 1445 | 2.56 | 5.05 | 2.34 | 4.62 |
| 521 | 60 | .1494 | 1400 | 2.49 | 5.09 | 2.28 | 4.65 |
| 516 | 80 | .1863 | 1460 | 2.33 | 4.55 | 2.13 | 4.17 |
| 520 | 120 | .3168 | 1410 | 2.64 | 5.35 | 2.42 | 4.90 |

TABLE 8
### SUMMARY OF MASS RATE DATA

| | | |
|---|---|---|
| Specimen Dia. | 1" | Notes - |
| Specimen Mat'l | ATJ | (1) Unmodified data |
| Nozzle Exit Dia. | 5" | (2) Data modified for |
| Stag'n Press., atm | $7.00 \times 10^{-3}$ | Reynolds No. Effects |
| Enthalpy Ratio | 160 | $\triangledown$ Symbol on graphs |
| Reynolds No., $Re_s$ | 51 | |

| Run Nos. | Time Sec. | Mass Loss $Lb/ft.^2$ | Avg. $^\circ K$ Temp. | Mass Rate $\times 10^3$ $lb/ft^2$ - sec (1) | (2) | $\dot{m}\sqrt{\dfrac{Rb}{Pe}} \times 10^3$ $lb/ft^{3/2}$-sec-Atm$^{1/2}$ (1) | (2) |
|---|---|---|---|---|---|---|---|
| 631 | 1200 | 1.2195 | 1280 | 1.02 | 1.042 | 3.90 | 3.98 |
| 631 | 1200 | 1.2195 | | | | | |
| 634 | 240 | .2232 | | | | | |
| | 960 | .9963 | 1270 | 1.04 | 1.09 | 3.975 | 4.165 |
| 631 | 1200 | 1.2195 | | | | | |
| 642 | 310 | .2305 | | | | | |
| | 890 | .9890 | 1280 | 1.11 | 1.134 | 4.24 | 4.34 |
| 631 | 1200 | 1.2195 | | | | | |
| 635 | 360 | .2979 | | | | | |
| | 840 | .9216 | 1285 | 1.10 | 1.123 | 4.21 | 4.29 |
| 631 | 1200 | 1.2195 | | | | | |
| 633 | 463 | .4626 | | | | | |
| | 737 | .7569 | 1260 | 1.03 | 1.090 | 3.94 | 4.165 |
| 631 | 1200 | 1.2195 | | | | | |
| 639 | 600 | .4707 | | | | | |
| | 600 | .7488 | 1285 | 1.25 | 1.278 | 4.77 | 4.89 |
| 631 | 1200 | 1.2195 | | | | | |
| 638 | 720 | .6138 | | | | | |
| | 480 | .6057 | 1275 | 1.26 | 1.307 | 4.82 | 5.00 |
| 631 | 1200 | 1.2195 | | | | | |
| 643 | 772 | .6462 | | | | | |
| | 428 | ..5733 | 1300 | 1.34 | 1.348 | 5.12 | 5.15 |
| 631 | 1200 | 1.2195 | | | | | |
| 644 | 801 | .7137 | | | | | |
| | 399 | .5058 | 1295 | 1.265 | 1.287 | 4.84 | 4.92 |
| 632 | 960 | .6930 | 1260 | 0.722 | .765 | 2.76 | 2.92 |

TABLE 8

SUMMARY OF MASS RATE DATA

| Specimen Dia. | 1" | Notes - |
|---|---|---|
| Specimen Mat'l | ATJ | (1) Unmodified data |
| Nozzle Exit Dia. | 5" | (2) Data modified for |
| Stag'n Press., atm | $7.00 \times 10^{-3}$ | Reynolds No. Effects |
| Enthalpy Ratio | 160 | $\triangledown$ Symbol on graphs |
| Reynolds No., $Re_s$ | 51 | |

| Run Nos. | Time Sec. | Mass Loss Lb/ft.$^2$ | Avg. $^{\circ}$K Temp. | Mass Rate $\times 10^3$ lb/ft$^2$ - sec (1) | (2) | $\dot{m}\sqrt{\dfrac{Rb}{Pe}} \times 10^3$ lb/ft$^{3/2}$-sec-Atm$^{1/2}$ (1) | (2) |
|---|---|---|---|---|---|---|---|
| 632 | 960 | .6930 | | | | | |
| 634 | 240 | .2232 | | | | | |
| | 720 | .4698 | 1255 | 0.653 | .695 | 2.66 | 3.045 |
| 632 | 960 | .6930 | | | | | |
| 642 | 310 | .2305 | | | | | |
| | 650 | .4625 | 1260 | 0.713 | .765 | 2.725 | 2.925 |
| 632 | 960 | .6930 | | | | | |
| 635 | 360 | .2979 | | | | | |
| | 600 | .3951 | 1270 | 0.658 | .690 | 2.515 | 2.64 |
| 632 | 960 | .6930 | | | | | |
| 633 | 463 | .4626 | | | | | |
| | 497 | .2304 | 1245 | 0.464 | .481 | 1.773 | 1.84 |
| 632 | 960 | .6930 | | | | | |
| 641 | 480 | .4104 | | | | | |
| | 480 | .2826 | 1275 | 0.589 | .610 | 2.25 | 2.33 |
| 632 | 960 | .6930 | | | | | |
| 639 | 600 | .4707 | | | | | |
| | 360 | .2223 | 1270 | 0.618 | .648 | 2.36 | 2.48 |
| 632 | 960 | .6930 | | | | | |
| 638 | 720 | .6138 | | | | | |
| | 240 | .0792 | 1260 | 0.330 | .350 | 1.262 | 1.339 |
| 632 | 960 | .6930 | | | | | |
| 643 | 772 | .6462 | | | | | |
| | 188 | .0468 | 1210 | 0.249 | .278 | .947 | 1.062 |
| 644 | 801 | .7137 | 1265 | 0.890 | .938 | 3.405 | 3.585 |
| 644 | 801 | .7137 | | | | | |
| 634 | 240 | .2232 | | | | | |
| | 561 | .4905 | 1325 | 0.885 | .860 | 3.38 | 3.285 |

TABLE 8
SUMMARY OF MASS RATE DATA

| | | Notes - |
|---|---|---|
| Specimen Dia. | 1" | (1) Unmodified data |
| Specimen Mat'l | ATJ | (2) Data modified for |
| Nozzle Exit Dia. | 5" | Reynolds No. Effects |
| Stag'n Press., atm | $7.00 \times 10^{-3}$ | $\nabla$ Symbol on graphs |
| Enthalpy Ratio | 160 | |
| Reynolds No., $Re_s$ | 51 | |

| Run Nos. | Time Sec. | Mass Loss Lb/ft.$^2$ | Avg. $^\circ$K Temp. | Mass Rate x 10$^3$ lb/ft$^2$ - sec (1) | (2) | $\dot{m}\sqrt{\dfrac{Rb}{Pe}} \times 10^3$ lb/ft$^{3/2}$-sec-Atm$^{1/2}$ (1) | (2) |
|---|---|---|---|---|---|---|---|
| 644 | 801 | .7137 | | | | | |
| 642 | 310 | .2305 | | | | | |
| | 491 | .4832 | 1255 | 0.985 | 1.048 | 3.76 | 4.00 |
| | | | | | | | |
| 644 | 801 | :7137 | | | | | |
| 635 | 360 | .2979 | | | | | |
| | 441 | .4158 | 1340 | 0.944 | .895 | 3.61 | 3.42 |
| | | | | | | | |
| 644 | 801 | .7137 | | | | | |
| 633 | 463 | .4626 | | | | | |
| | 338 | .2511 | 1315 | 0.744 | .733 | 2.85 | 2.91 |
| | | | | | | | |
| 644 | 801 | .7137 | | | | | |
| 641 | 480 | .4104 | | | | | |
| | 321 | .3033 | 1270 | 0.942 | .988 | 3.60 | 3.775 |
| | | | | | | | |
| 644 | 801 | .7137 | | | | | |
| 639 | 600 | .4707 | | | | | |
| | 201 | .2430 | 1340 | 1.210 | 1.147 | 4.62 | 4.38 |
| | | | | | | | |
| 644 | 801 | .7137 | | | | | |
| 638 | 720 | .6138 | | | | | |
| | 81 | .0999 | 1330 | 1.233 | 1.193 | 4.71 | 4.56 |
| | | | | | | | |
| 643 | 772 | .6462 | | | | | |
| 634 | 240 | .2232 | | | | | |
| | 532 | .4230 | 1280 | .795 | .820 | 3.04 | 3.135 |
| | | | | | | | |
| 643 | 772 | .6462 | | | | | |
| 642 | 310 | .2305 | | | | | |
| | 462 | .4157 | 1285 | .900 | .919 | 3.44 | 3.51 |
| | | | | | | | |
| 643 | 772 | .6462 | | | | | |
| 635 | 360 | .2979 | | | | | |
| | 412 | .3483 | 1295 | .845 | .854 | 3.23 | 3.265 |

## TABLE 8
### SUMMARY OF MASS RATE DATA

| Specimen Dia. | 1" | | Notes - |
|---|---|---|---|
| Specimen Mat'l | ATJ | | (1) Unmodified data |
| Nozzle Exit Dia. | 5" | | (2) Data modified for |
| Stag'n Press., atm | $7.00 \times 10^{-3}$ | | Reynolds No. Effects |
| Enthalpy Ratio | 160 | | ▽ Symbol on graphs |
| Reynolds No., $Re_s$ | 51 | | |

| Run Nos. | Time Sec. | Mass Loss Lb/ft.$^2$ | Avg. $^\circ$K Temp. | Mass Rate $\times 10^3$ lb/ft$^2$ - sec (1) | (2) | $\dot{m}\sqrt{\dfrac{Rb}{Pe}} \times 10^3$ lb/ft$^{3/2}$-sec-Atm$^{1/2}$ (1) | (2) |
|---|---|---|---|---|---|---|---|
| 643 | 772 | .6462 | | | | | |
| 633 | 463 | .4626 | | | | | |
| | 309 | .1836 | 1270 | .593 | .622 | 2.265 | 2.38 |
| | | | | | | | |
| 643 | 772 | .6462 | | | | | |
| 641 | 480 | .4104 | | | | | |
| | 292 | .2358 | 1225 | .807 | .893 | 3.085 | 3.42 |
| | | | | | | | |
| 643 | 772 | .6462 | | | | | |
| 639 | 600 | .4707 | | | | | |
| | 172 | .1755 | 1295 | 1.021 | 1.031 | 3.90 | 3.94 |
| | | | | | | | |
| 643 | 772 | .6462 | | | | | |
| 638 | 720 | .6138 | | | | | |
| | 52 | .0324 | 1285 | 0.623 | .637 | 2.38 | 2.44 |
| | | | | | | | |
| 638 | 720 | .6138 | 1225 | 0.853 | .943 | 3.26 | 3.60 |
| | | | | | | | |
| 638 | 720 | .6138 | | | | | |
| 634 | 240 | .2232 | | | | | |
| | 480 | .3906 | 1285 | 0.815 | .832 | 3.12 | 3.18 |
| | | | | | | | |
| 638 | 720 | .6138 | | | | | |
| 642 | 310 | .2305 | | | | | |
| | 410 | .3833 | 1290 | 0.935 | .949 | 3.575 | 3.63 |
| | | | | | | | |
| 638 | 720 | .6138 | | | | | |
| 635 | 360 | .2979 | | | | | |
| | 360 | .3159 | 1300 | 0.878 | .883 | 3.36 | 3.38 |
| | | | | | | | |
| 638 | 720 | .6138 | | | | | |
| 633 | 463 | .4626 | | | | | |
| | 257 | .1512 | 1275 | 0.588 | .609 | 2.25 | 2.325 |
| | | | | | | | |
| 638 | 720 | .6138 | | | | | |
| 641 | 480 | .4104 | | | | | |
| | 240 | .1034 | 1230 | 0.432 | .494 | 1.65 | 1.89 |

## TABLE 8
### SUMMARY OF MASS RATE DATA

| | | |
|---|---|---|
| Specimen Dia. | 1" | |
| Specimen Mat'l | ATJ | |
| Nozzle Exit Dia. | 5" | |
| Stag'n Press., atm | $7.00 \times 10^{-3}$ | |
| Enthalpy Ratio | 160 | |
| Reynolds No., $Re_s$ | 51 | |

Notes -
(1) Unmodified data
(2) Data modified for Reynolds No. Effects
▽ Symbol on graphs

| Run Nos. | Time Sec. | Mass Loss Lb/ft.$^2$ | Avg. °K Temp. | Mass Rate $\times 10^3$ lb/ft$^2$ - sec (1) | (2) | $\dot{m}\sqrt{\dfrac{Rb}{Pe}} \times 10^3$ lb/ft$^{3/2}$-sec-Atm$^{1/2}$ (1) | (2) |
|---|---|---|---|---|---|---|---|
| 638 | 720 | .6138 | | | | | |
| 639 | 600 | .4707 | | | | | |
| | 120 | .1431 | 1300 | 1.190 | 1.197 | 4.55 | 4.57 |
| 642 | 310 | .2305 | 1250 | 0.745 | .798 | 2.85 | 3.05 |
| 639 | 600 | .4707 | 1245 | 0.785 | .849 | 3.00 | 3.24 |
| 639 | 600 | .4707 | | | | | |
| 634 | 240 | .2232 | | | | | |
| | 360 | .2475 | 1295 | 0.688 | .695 | 2.63 | 2.66 |
| 639 | 600 | .4707 | | | | | |
| 642 | 310 | .2305 | | | | | |
| | 290 | .2402 | 1225 | 0.829 | .917 | 3.17 | 3.51 |
| 639 | 600 | .4707 | | | | | |
| 635 | 360 | .2979 | | | | | |
| | 240 | .1728 | 1320 | 0.720 | .703 | 2.75 | 2.69 |
| 639 | 600 | .4707 | | | | | |
| 641 | 480 | .4104 | | | | | |
| | 120 | .0603 | 1240 | 0.504 | .549 | 1.927 | 2.10 |
| 641 | 480 | .4104 | 1255 | 0.855 | .911 | 3.27 | 3.48 |
| 641 | 480 | .4104 | | | | | |
| 634 | 240 | .2232 | | | | | |
| | 240 | .1872 | 1270 | 0.780 | .817 | 2.98 | 3.125 |
| 641 | 480 | .4104 | | | | | |
| 642 | 310 | .2305 | | | | | |
| | 170 | .1799 | 1275 | 1.068 | 1.108 | 4.08 | 4.23 |
| 641 | 480 | .4104 | | | | | |
| 635 | 360 | .2979 | | | | | |
| | 120 | .1125 | 1285 | 0.938 | .958 | 3.585 | 3.66 |

TABLE 8
SUMMARY OF MASS RATE DATA

| Specimen Dia. | 1" |
| Specimen Mat'l | ATJ |
| Nozzle Exit Dia. | 5" |
| Stag'n Press., atm | $7.00 \times 10^{-3}$ |
| Enthalpy Ratio | 160 |
| Reynolds No., $Re_s$ | 51 |

Notes -
(1) Unmodified data
(2) Data modified for Reynolds No. Effects
$\triangledown$  Symbol on graphs

| Run Nos. | Time Sec. | Mass Loss Lb/ft.$^2$ | Avg. $^oK$ Temp. | Mass Rate $\times 10^3$ lb/ft$^2$ – sec (1) | (2) | $\dot{m}\sqrt{\dfrac{Rb}{Pe}} \times 10^3$ lb/ft$^{3/2}$-sec-Atm$^{1/2}$ (1) | (2) |
|---|---|---|---|---|---|---|---|
| 635 | 360 | .2979 | 1245 | 0.829 | .899 | 3.17 | 3.44 |
| 635 | 360 | .2979 | | | | | |
| 642 | 240 | .2232 | | | | | |
| | 120 | .0747 | 1290 | 0.623 | .569 | 2.38 | 2.175 |
| 635 | 360 | .2979 | | | | | |
| 634 | 310 | .2305 | | | | | |
| | 50 | .0674 | 1285 | 1.347 | 1.374 | 5.14 | 5.25 |
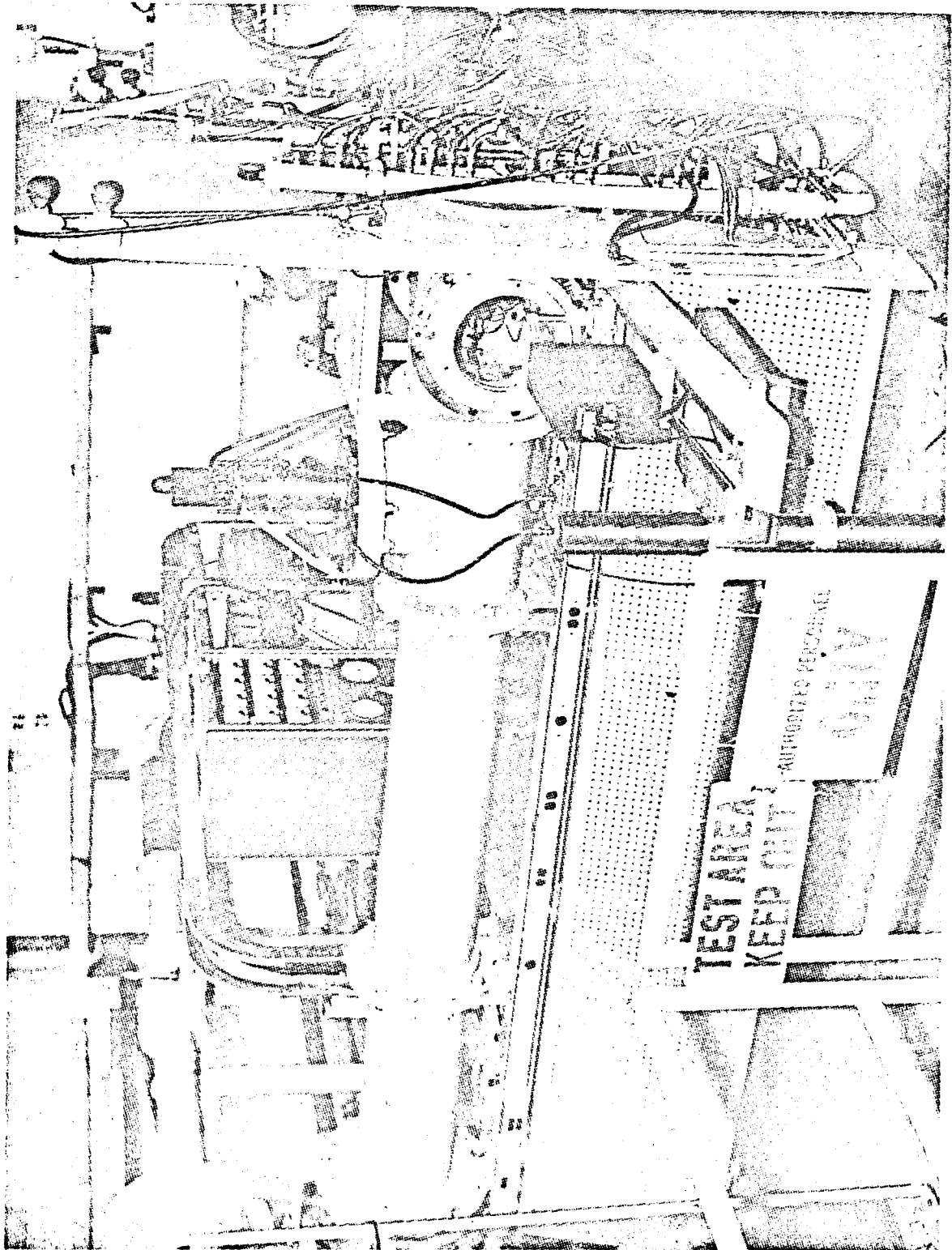
FIGURE 1  HYPERSONIC ARC HEATED WIND TUNNEL
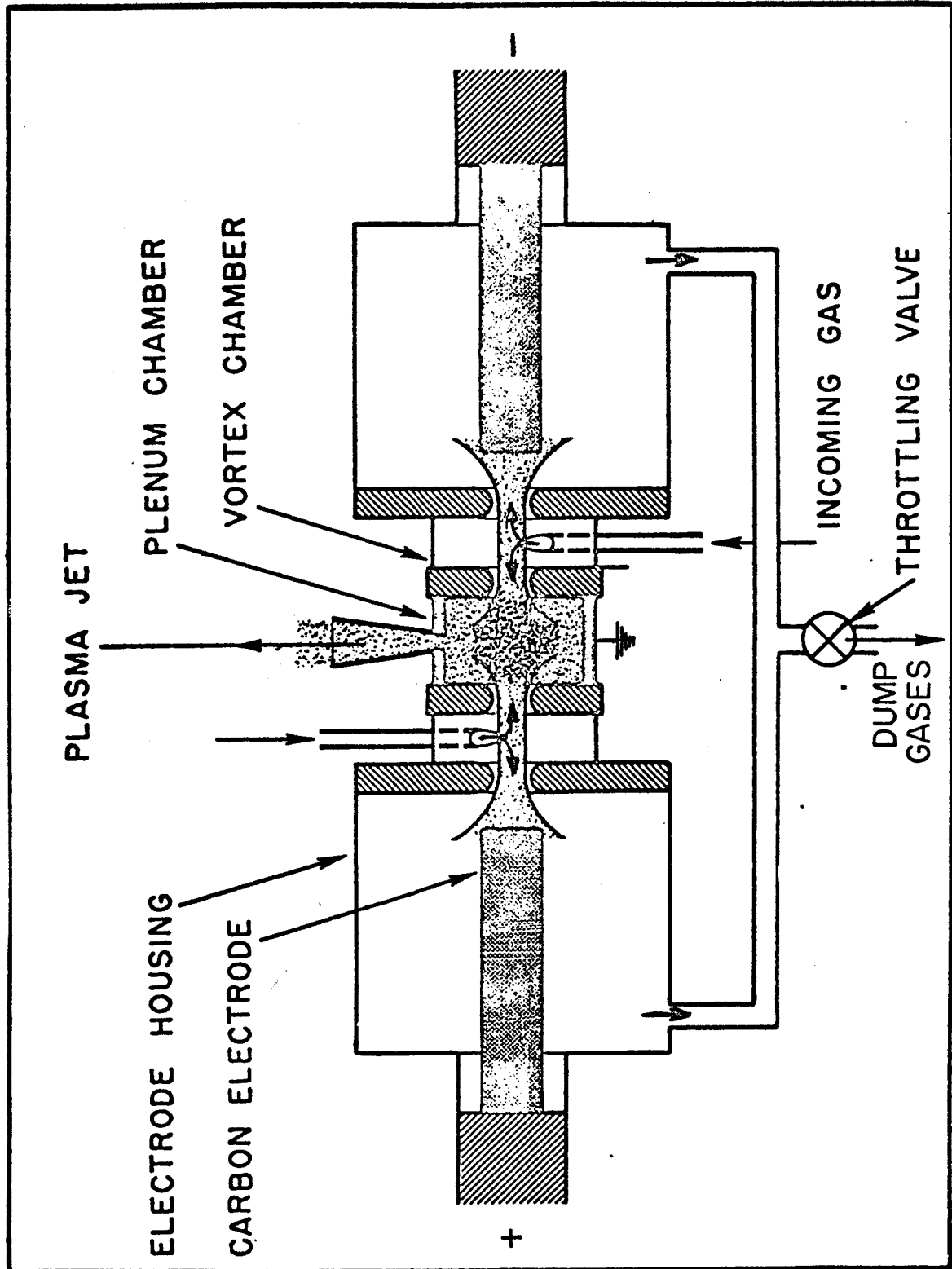
FIGURE 2 GENERAL ARRANGEMENT OF THE TANDEM GERDIEN PLASMA JET APPARATUS FOR ARC TUNNEL

GAS
+
CONT.

ELECTRODE
HOUSING

+

MODEL
OUT

GAS
IN

PLENUM

MODEL IN

BY-PASS
PORT

VORTEX
CHAMBER

GAS
IN

−

GAS
+
CONT.

GRAPHITE
ELECTRODE
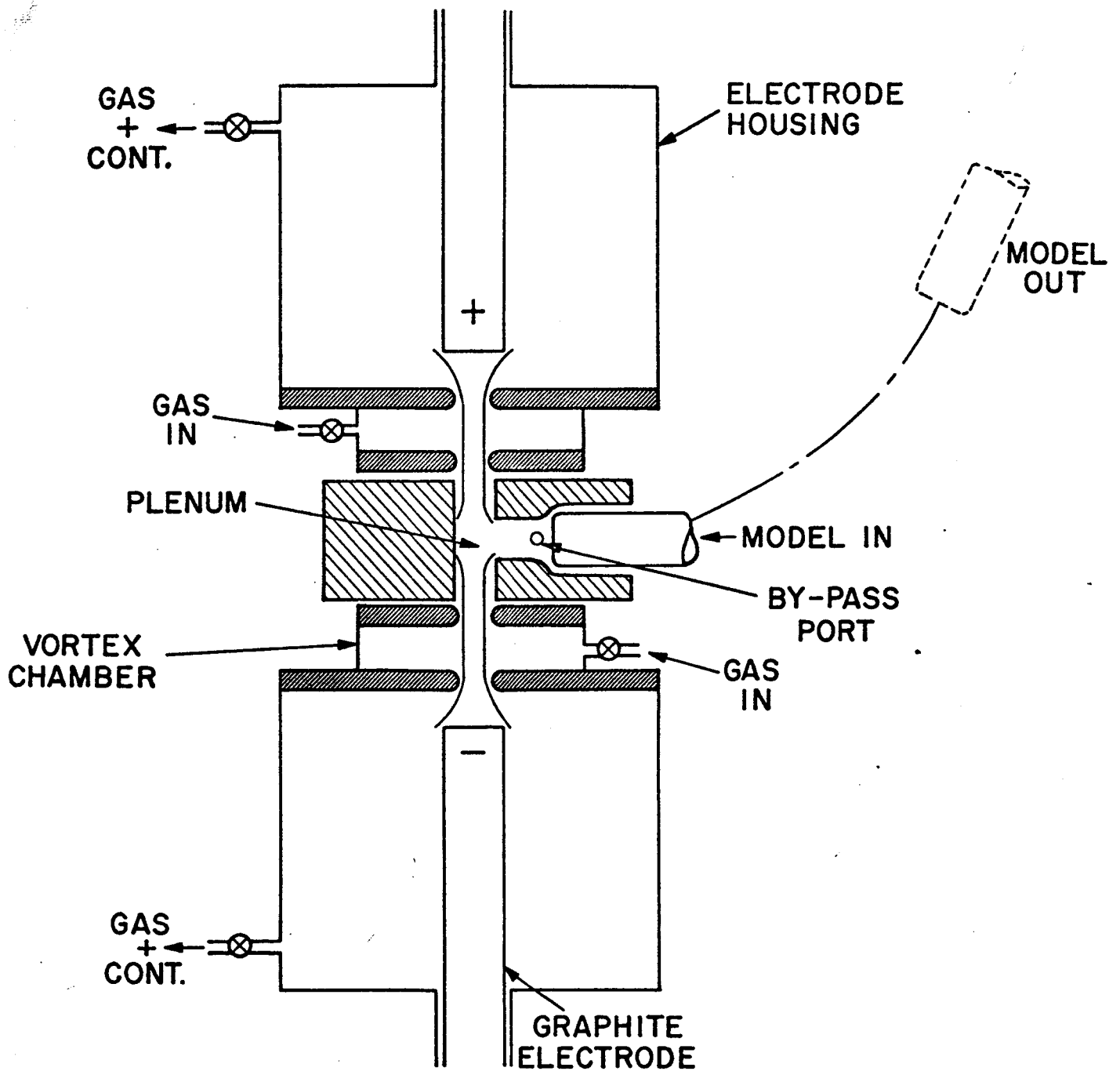
Figure 3a    GENERAL ARRANGEMENT TANDEM GERDIEN  FREE JET

EXHAUST FLOW COOLER

ELECTRODE HOUSING

PLENUM

VORTEX CHAMBER

ELECTRODE VIEW PORT
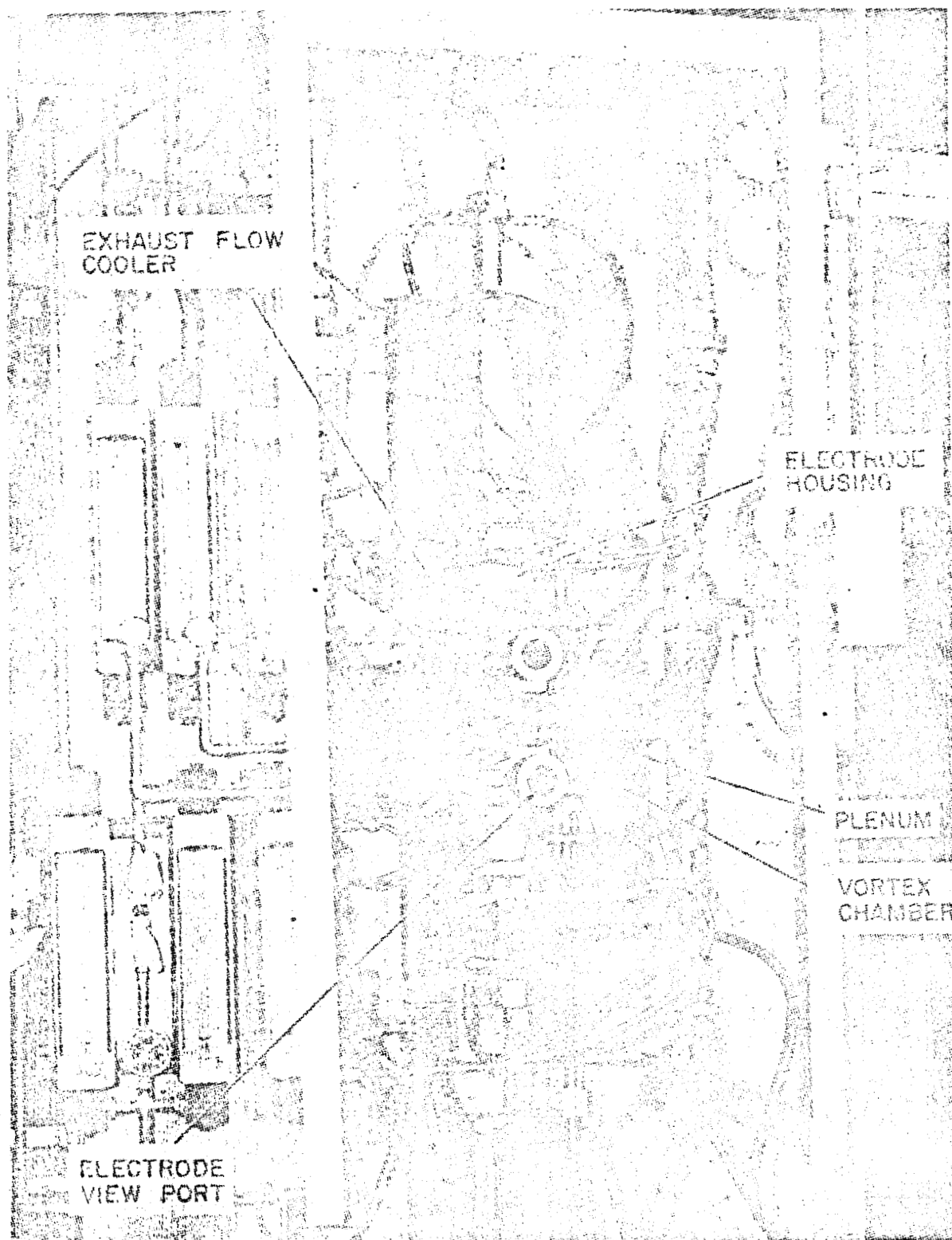
Figure 3b Tandem Gerdien Free Jet Arc Facility
Showing Arc Heater Equipment
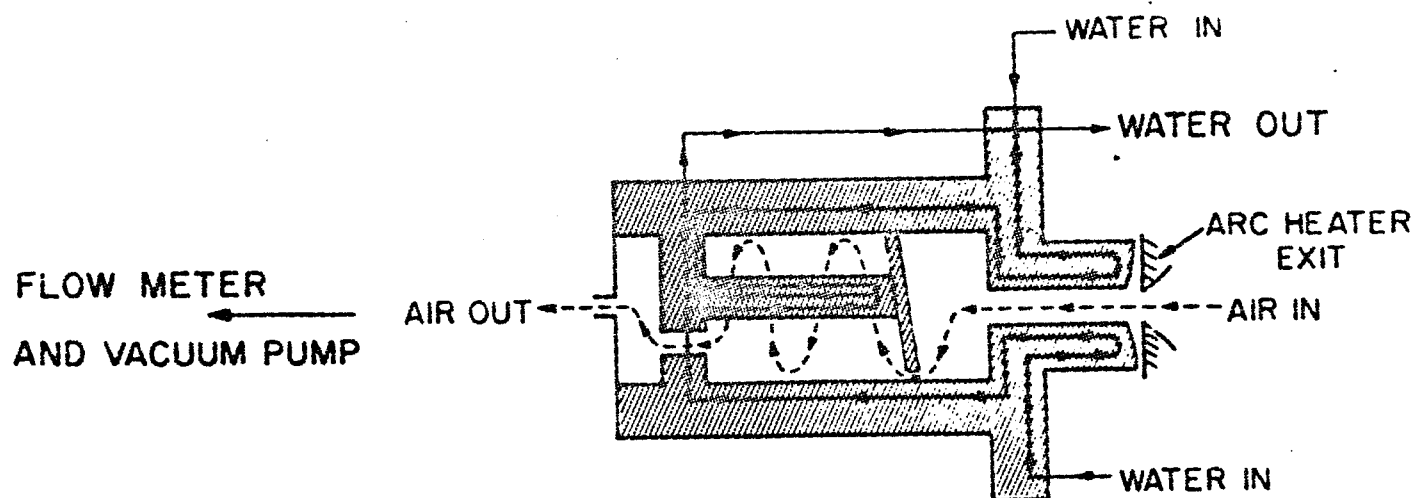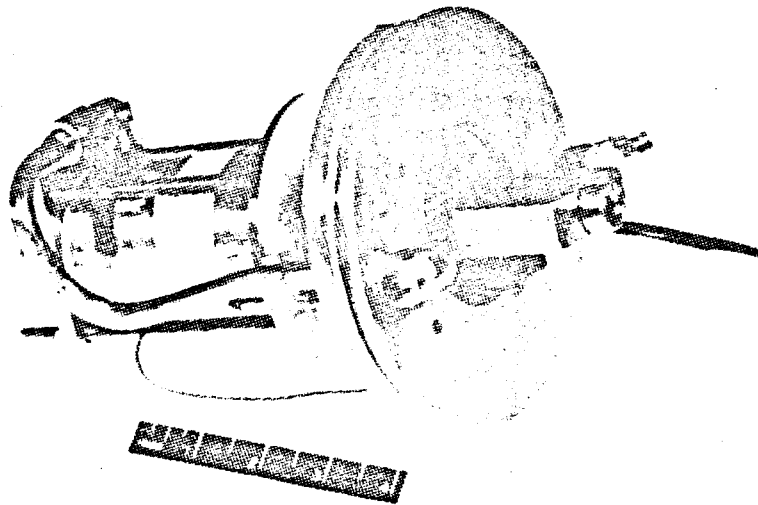
FIGURE 4    TOTAL ENTHALPY CALORIMETER FOR ARC TUNNEL

SEAL

NOZZLE INSERT

SEAL

PLENUM

CALORIMETER
INSERT
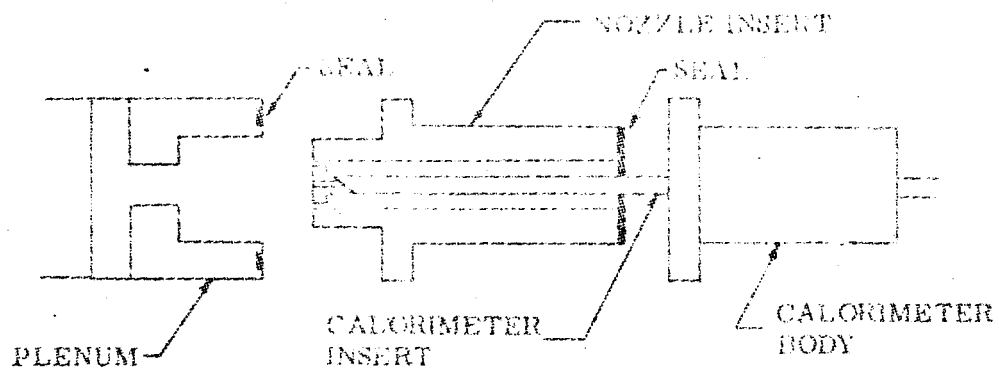
CALORIMETER
BODY

Figure 5 Total Enthalpy Calorimeter Tandem Gerdien **Free Jet Arc**
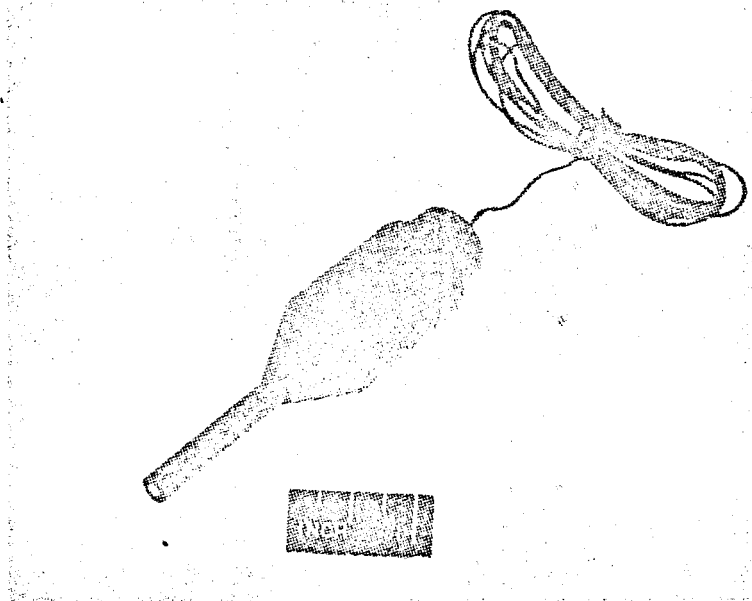
FIGURE 6   TYPICAL MASS TRANSFER MODEL CALORIMETER
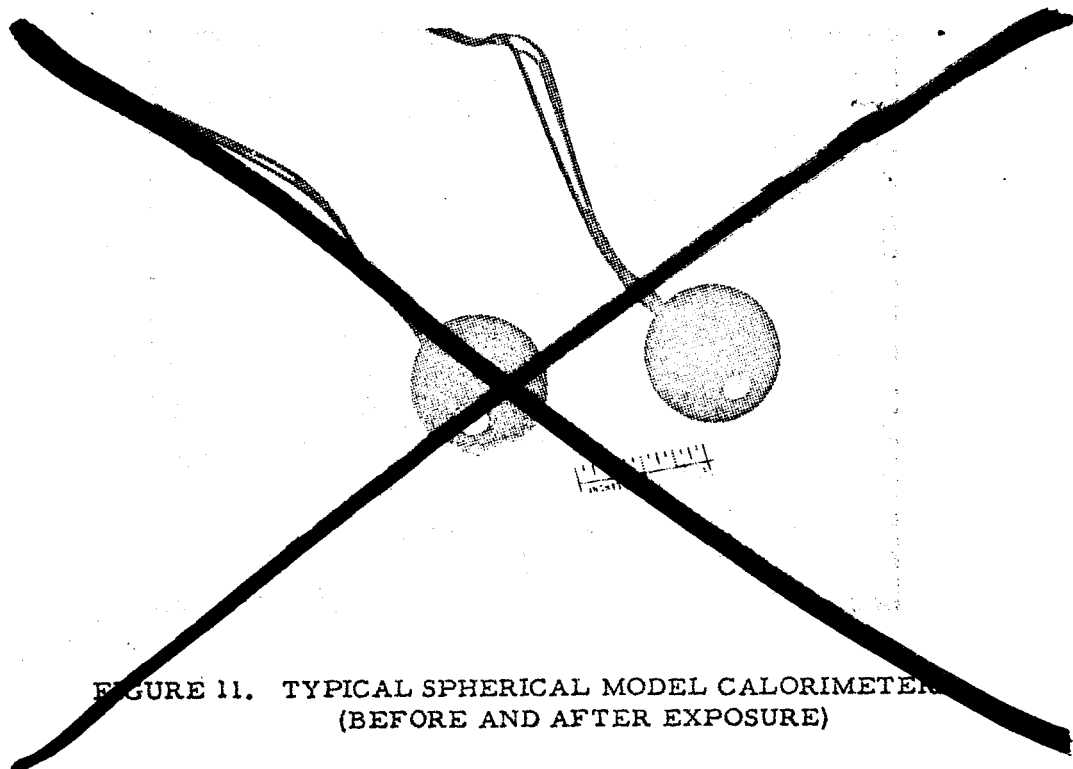


FIGURE 11.   TYPICAL SPHERICAL MODEL CALORIMETER
(BEFORE AND AFTER EXPOSURE)
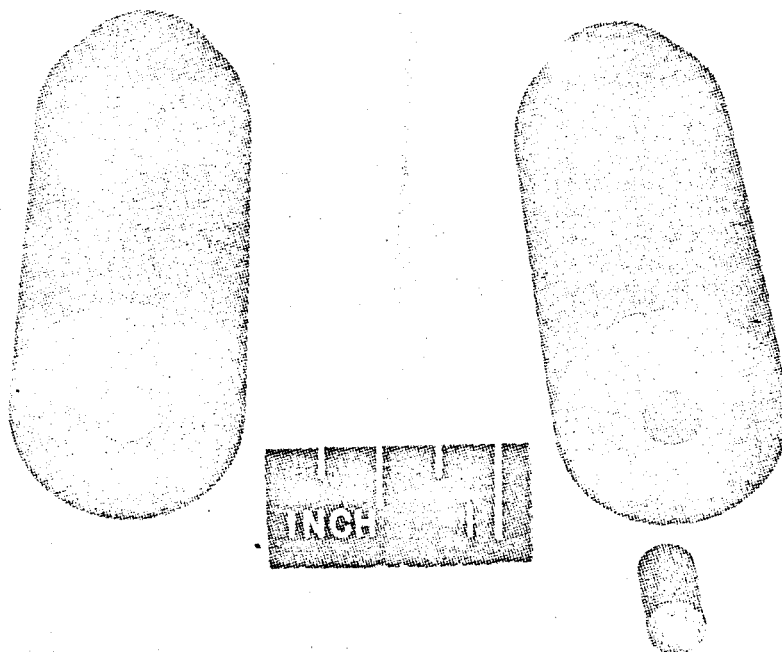
Figure 7a-1    MASS RATE SPECIMEN, 1.0" DIAMETER
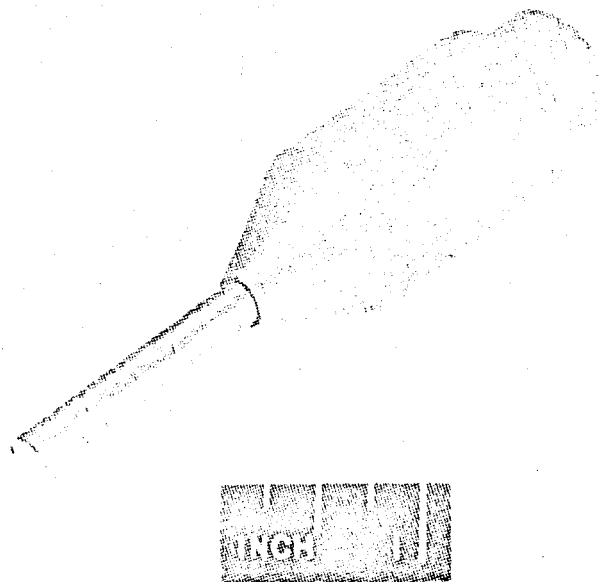


Figure 7a-2    MASS RATE SPECIMEN, 1/4" DIAMETER
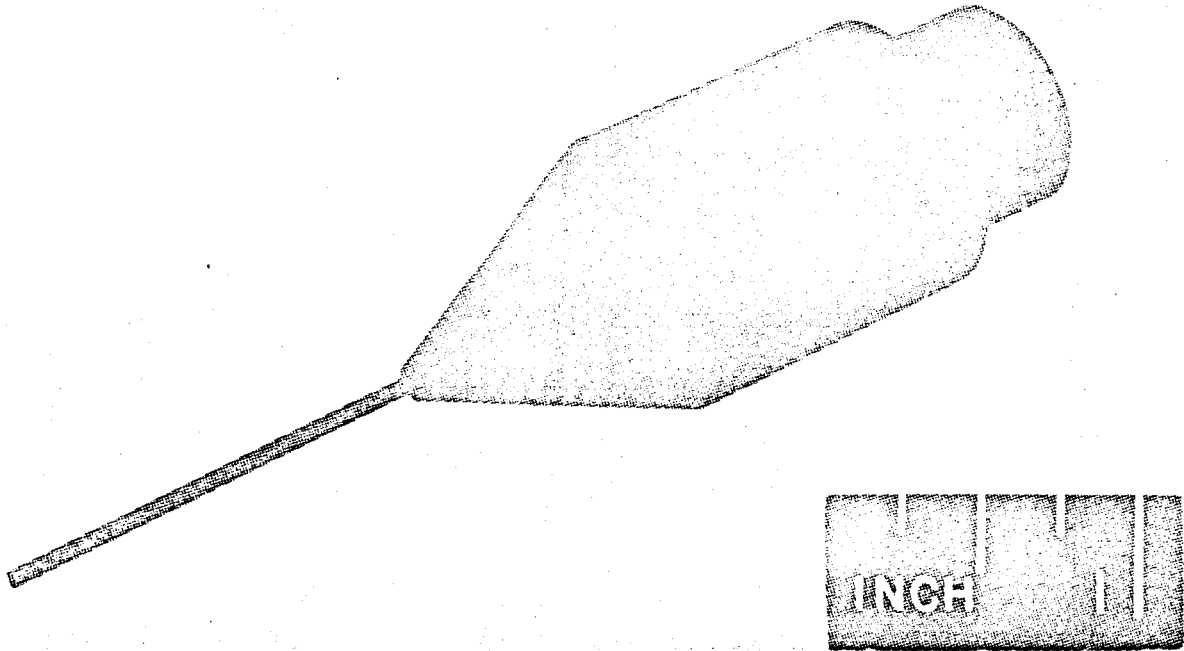
Figure 7a-3    MASS RATE SPECIMEN, 1/16" DIAMETER
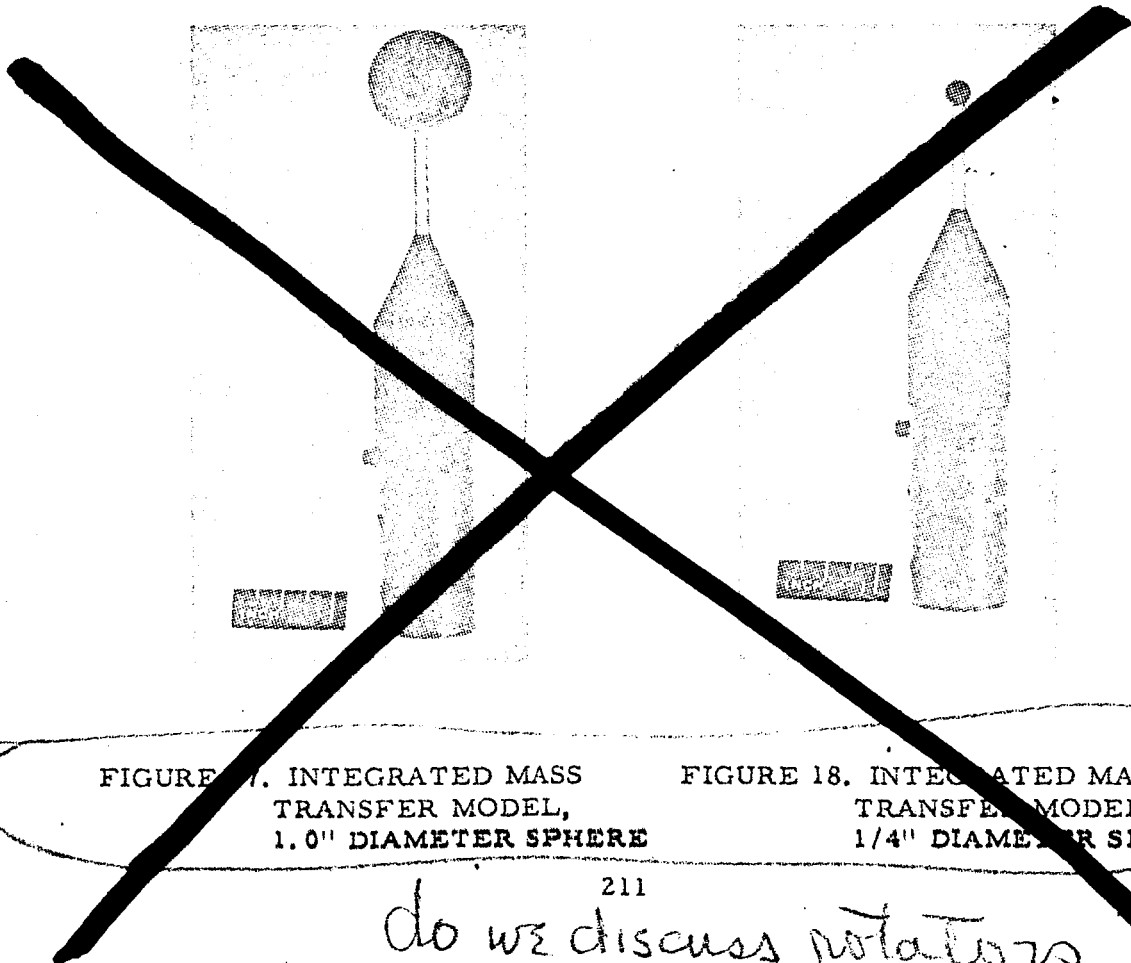


FIGURE 17. INTEGRATED MASS
TRANSFER MODEL,
1.0" DIAMETER SPHERE

FIGURE 18. INTEGRATED MASS
TRANSFER MODEL,
1/4" DIAMETER SPHERE

211

do we discuss protators

## MODIFICATIONS OF ATJ GRAPHITE SPECIMENS

### $\frac{1}{4}$ IN. DIA. MODELS

ITEM 17   FIG. 12



$1\frac{7}{16}$

.750

.250 DIA. — — — .147 DIA.   _a_

$1\frac{7}{16}$

.125

.250 DIA. — — — .147 DIA.   _b_

1"

.125
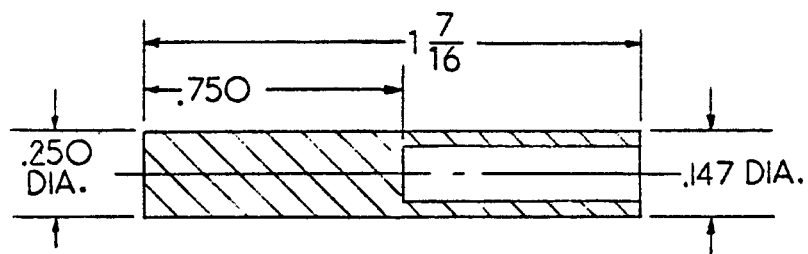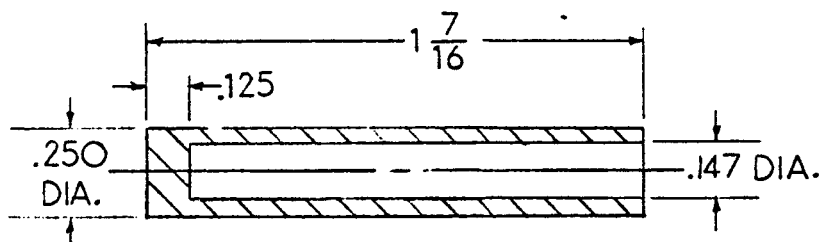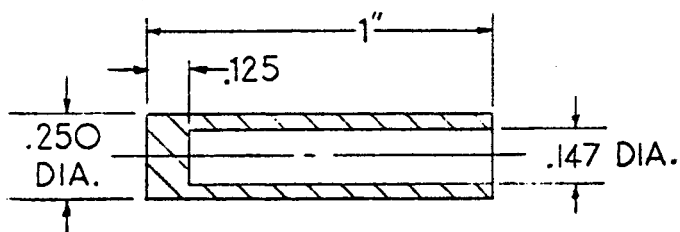
.250 DIA. — — — .147 DIA.   _c_

### $\frac{1}{16}$ IN. DIA. MODEL

ITEM 21   FIG. 12

2"

.125

.055 DIA.

.062 DIA.

CEMENT

ATJ

CERAMIC

_d_

FIGURE 7b

BASE

INSERT

GRAPHITE
MODEL BODY

P.G. SPECIMEN

ASSEMBLED
MODEL
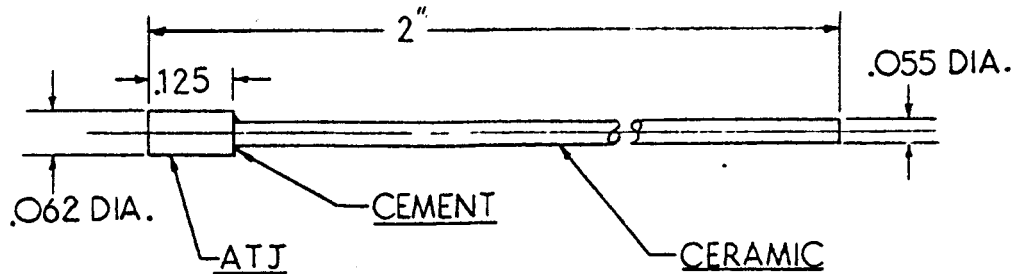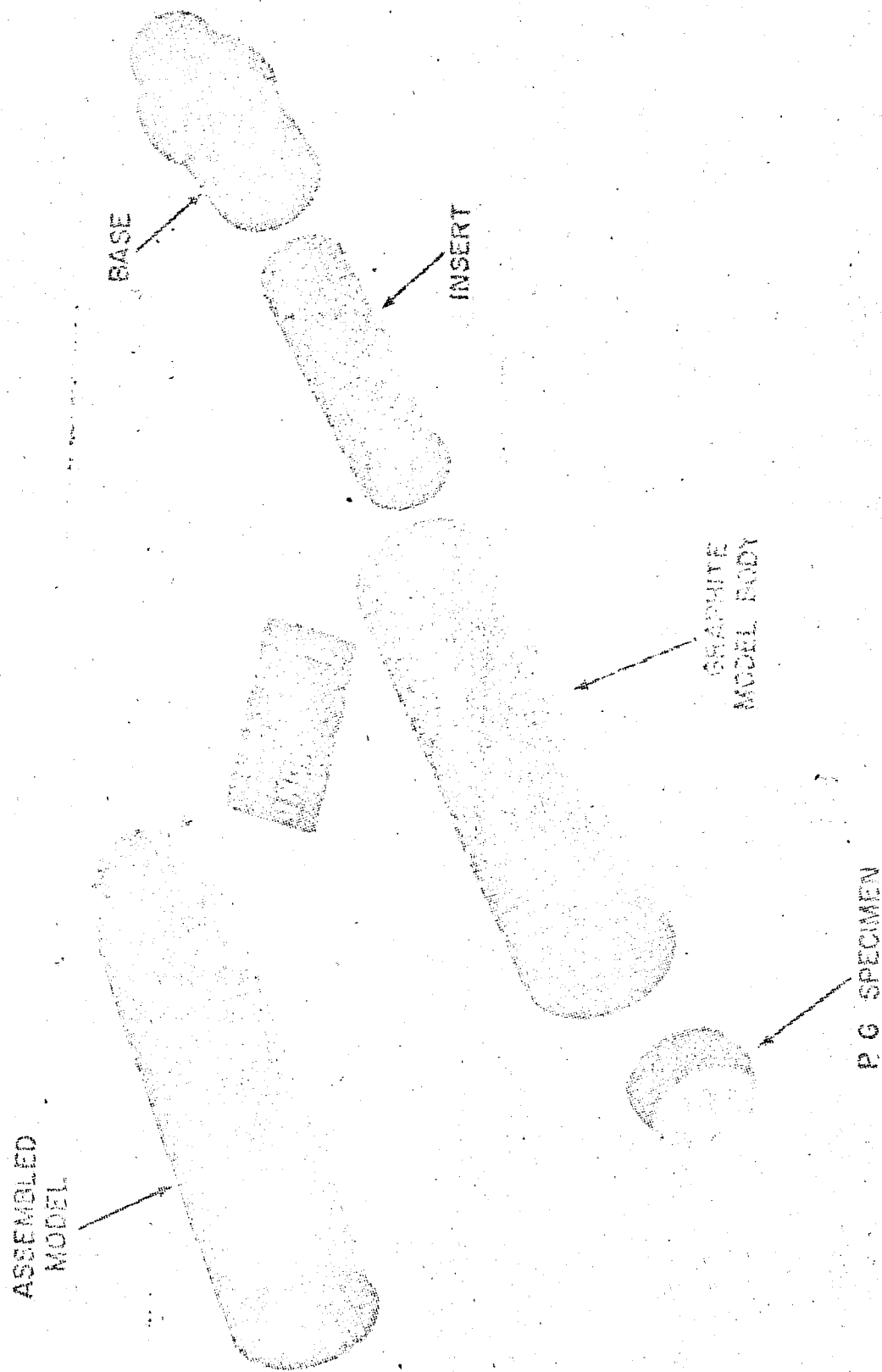
Figure 7c   Model used in fire jet tests
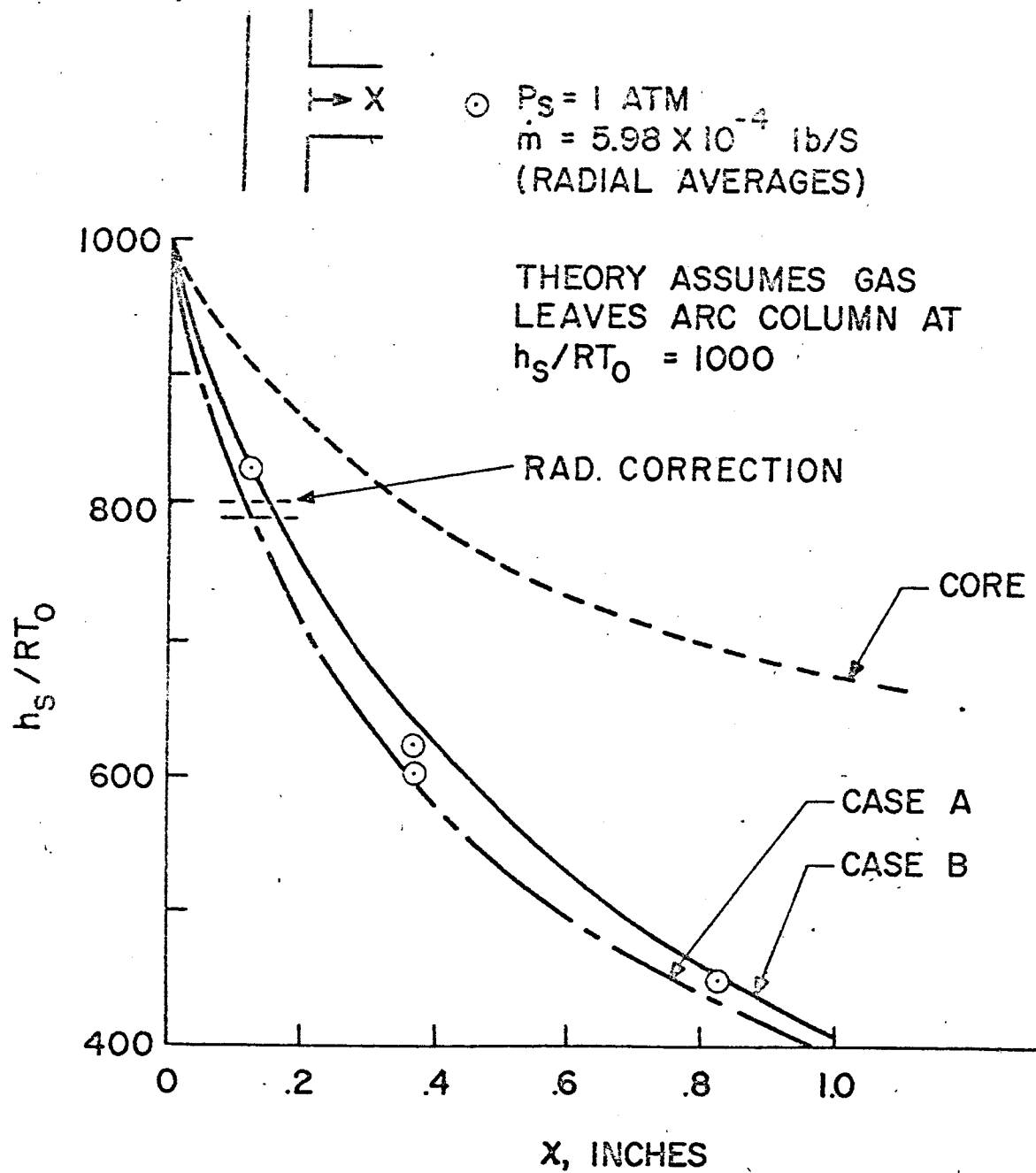
Figure 8.   Comparison of experimental and theoretical
stagnation enthalpy levels
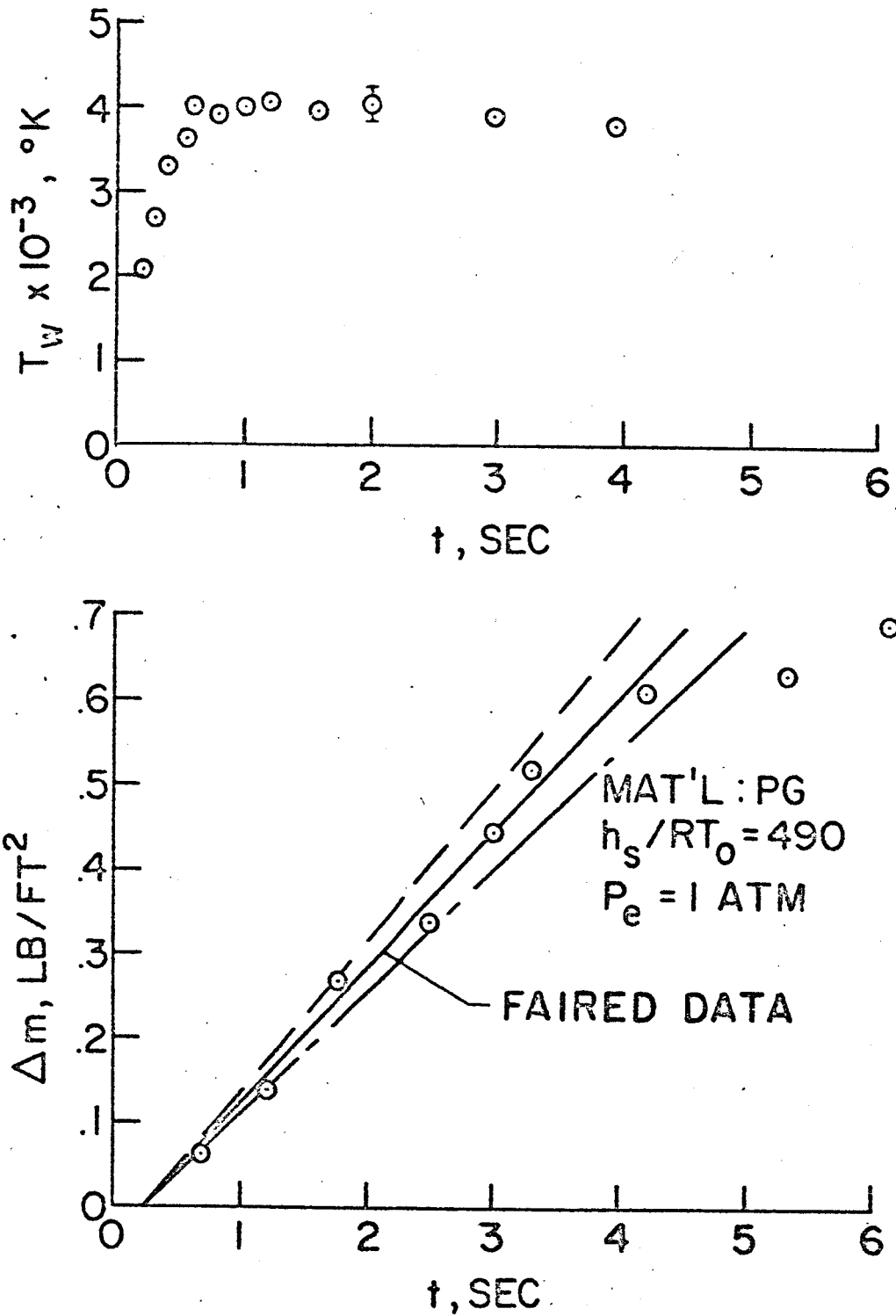
Figure 9a   Surface temperature and mass loss measurements
for free jet tests of pyrolytic graphite - high enthalpy
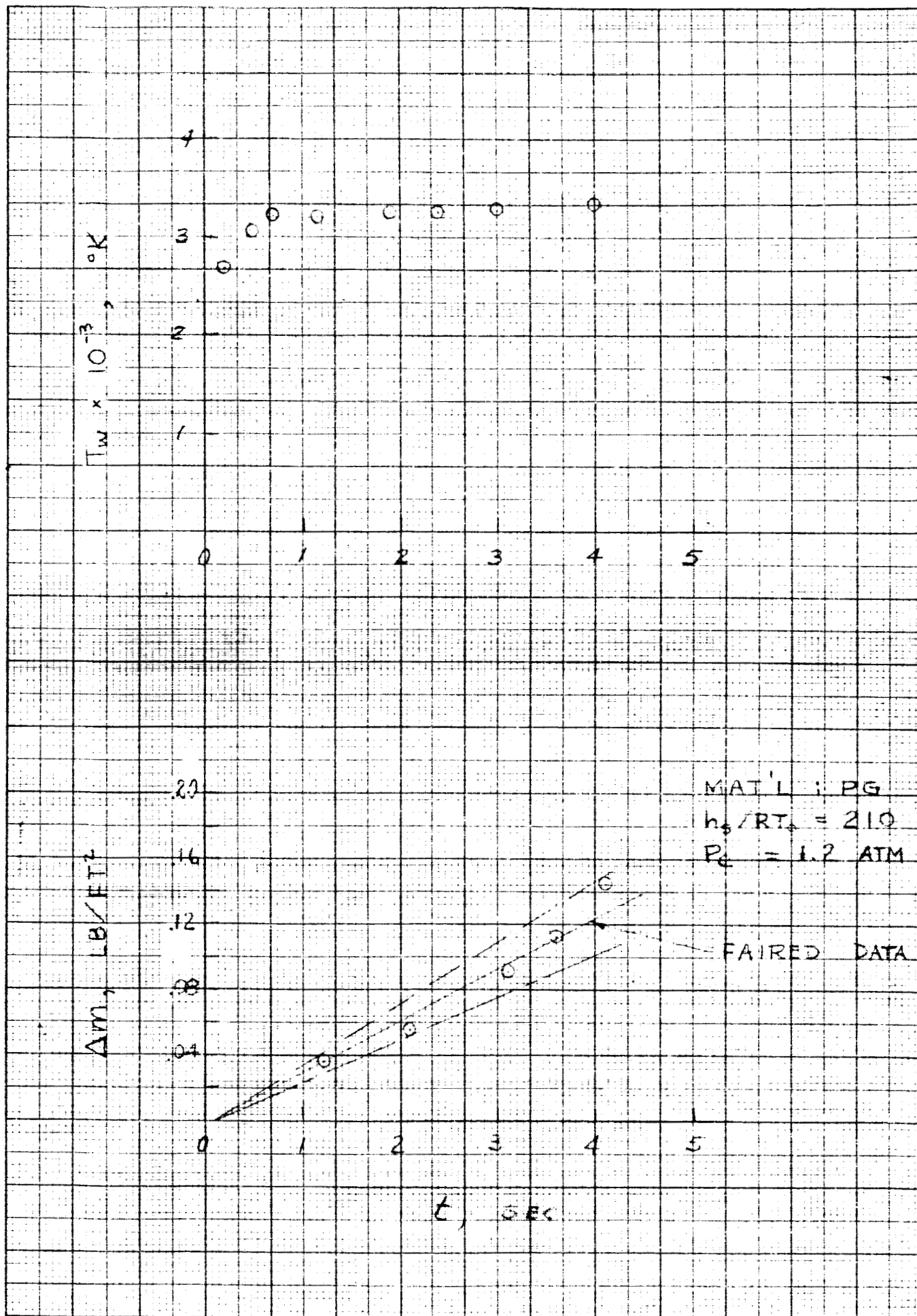
Figure 9b – Surface temperature and mass loss measurements for free jet
tests of pyrolytic graphite - low enthalpy
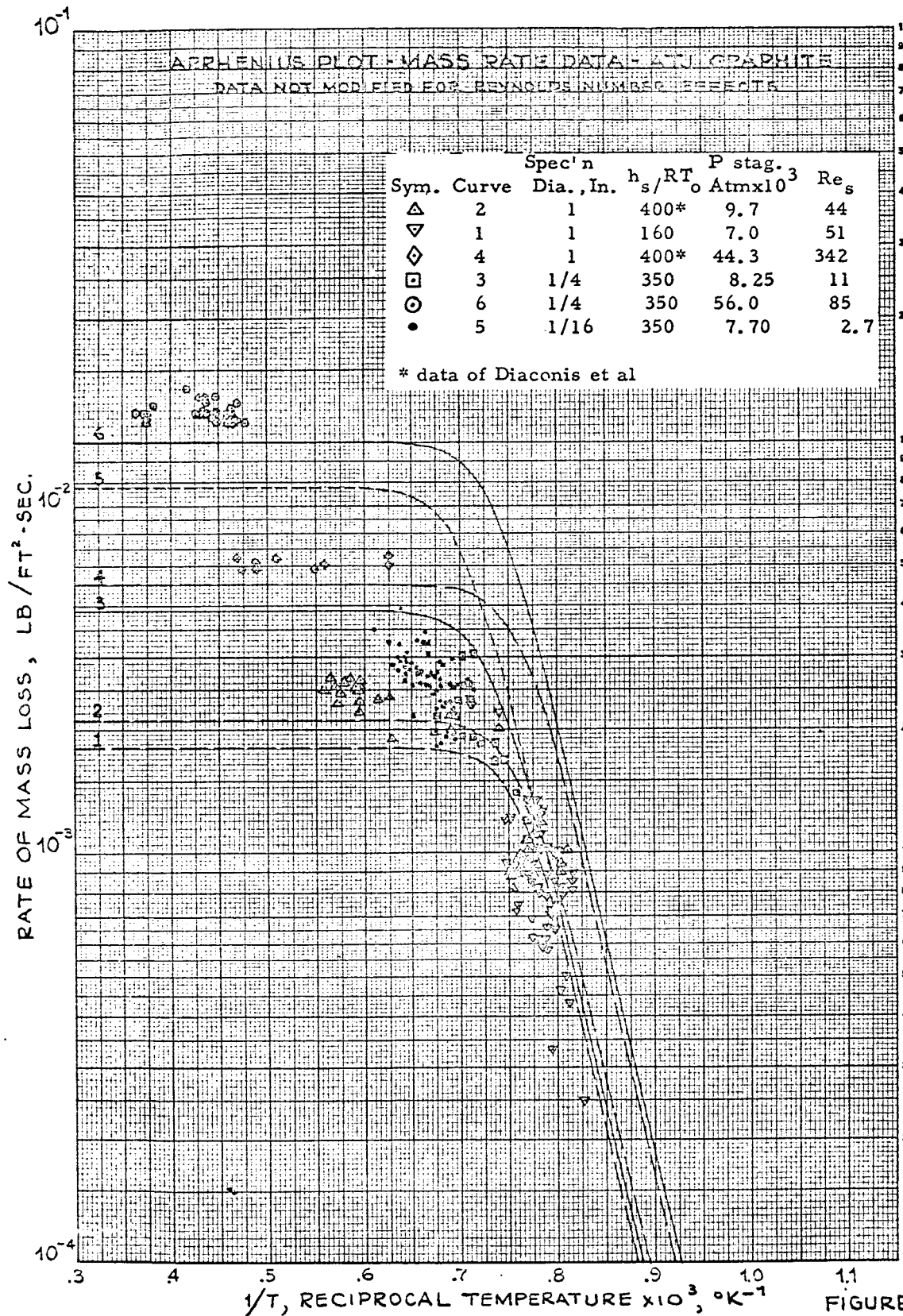
FIGURE 11

# FLOW REGIME CORRELATION FUNCTION
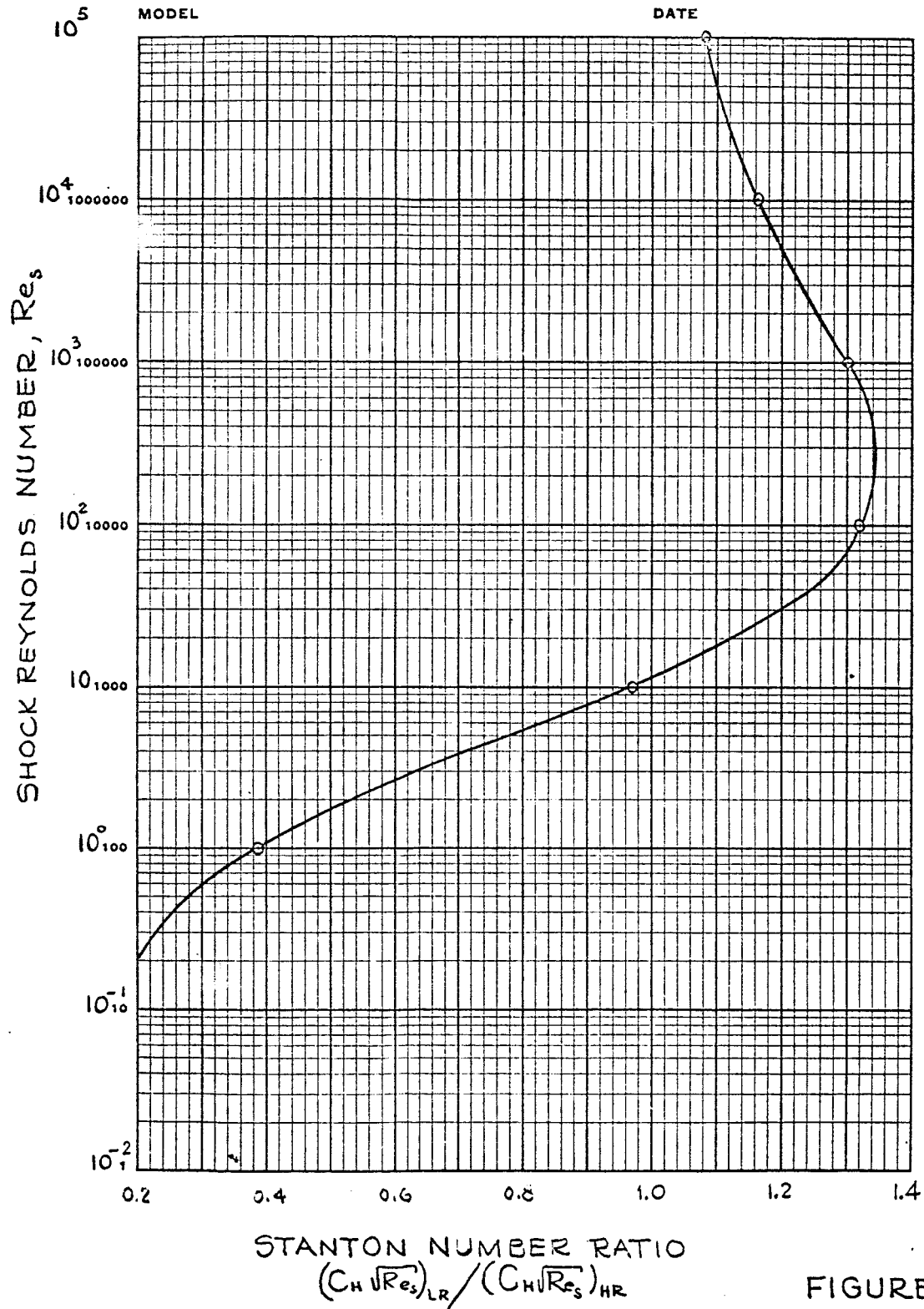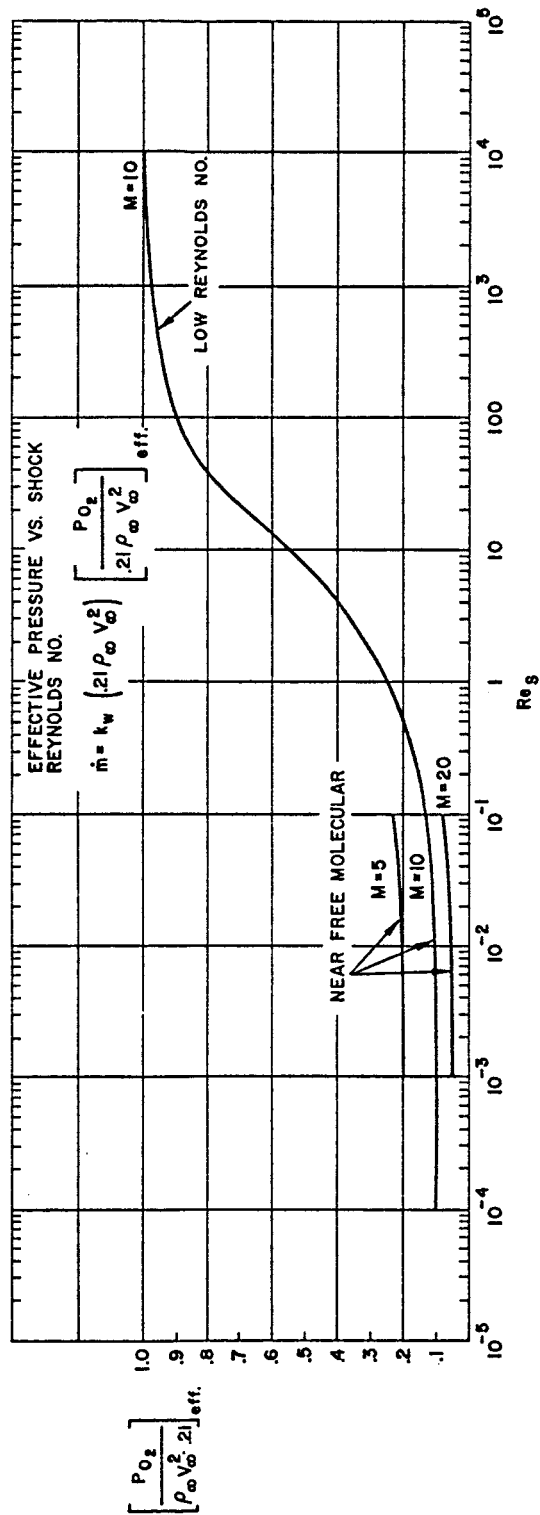


STANTON NUMBER RATIO
$$\left(C_H \sqrt{Re_s}\right)_{LR} / \left(C_H \sqrt{Re_s}\right)_{HR}$$

FIGURE 12

EFFECTIVE PRESSURE VS. SHOCK REYNOLDS NO.

$$\dot{m} = k_w \left(.21 \rho_\infty V_\infty^2\right) \left[\frac{P_{O_2}}{.21 \rho_\infty V_\infty^2}\right]_{eff.}$$

LOW REYNOLDS NO.

M=10

NEAR FREE MOLECULAR

M=5
M=10
M=20

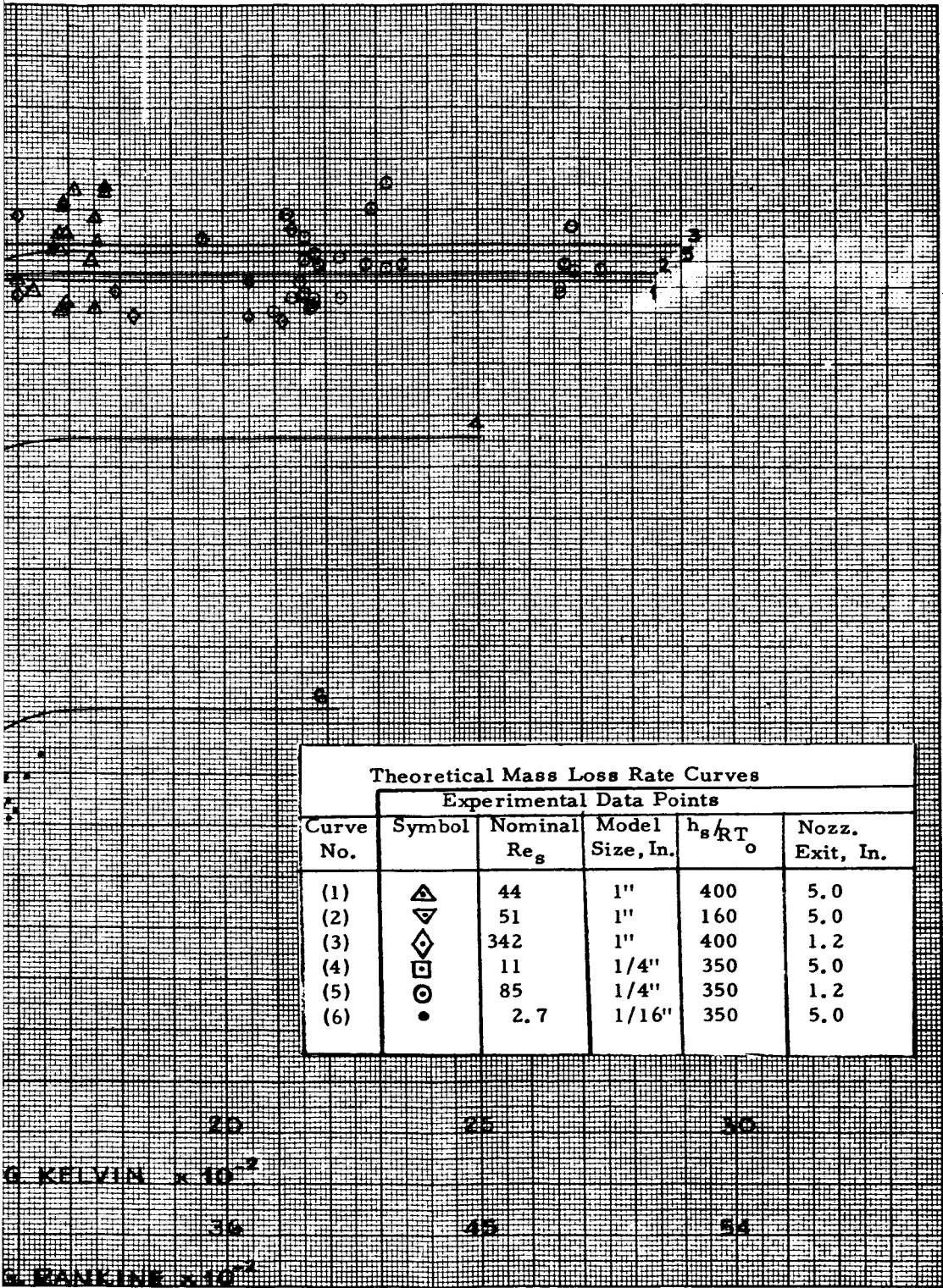$$\left[\frac{P_{O_2}}{\rho_\infty V_\infty^2 \cdot .21}\right]_{eff.}$$

$Re_s$
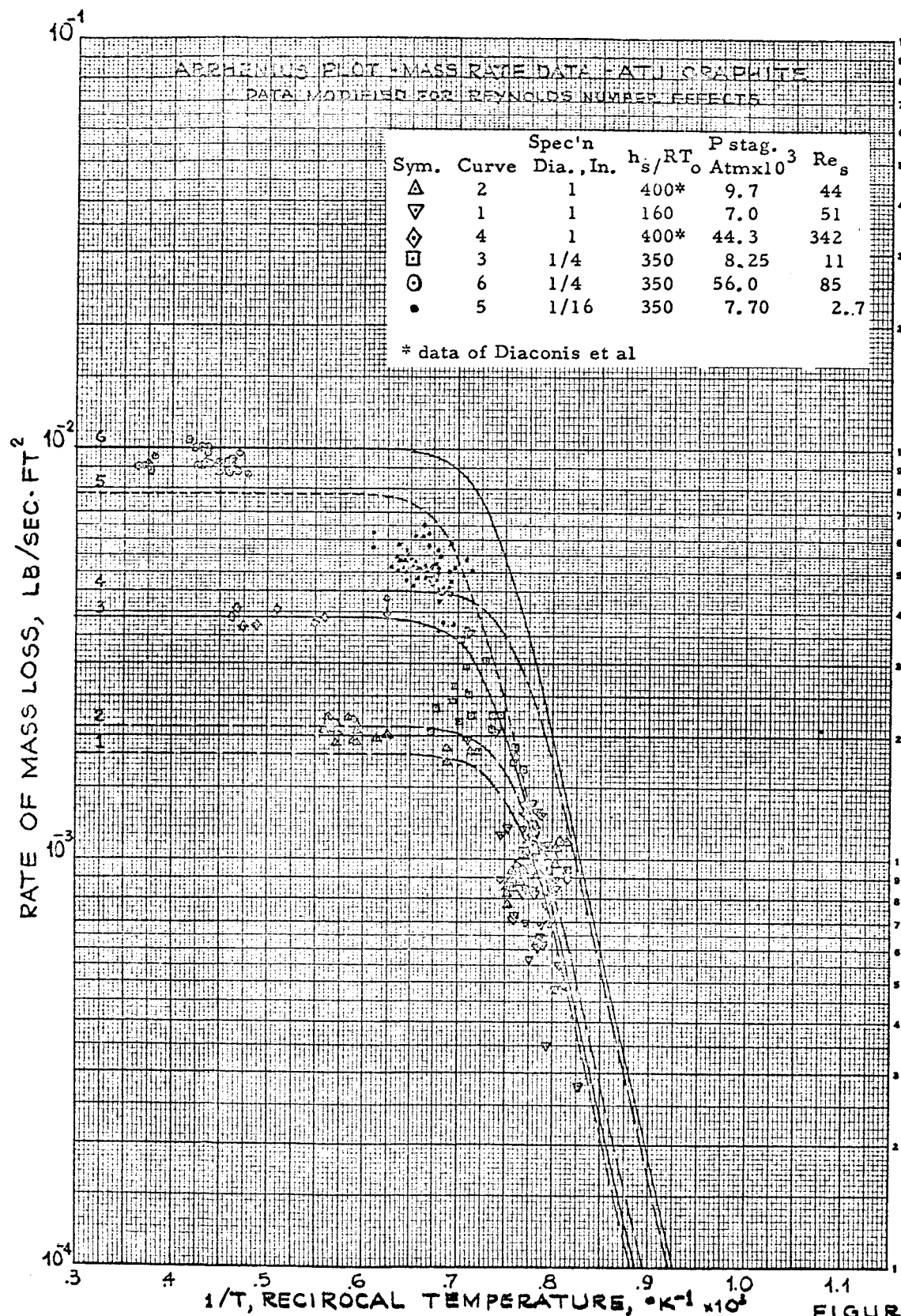
FIGURE 13

FIGURE 14

OXIDATION MASS RATE VS. SURFACE
TEMPERATURE FOR ATJ GRAPHITE

Data Obtained one-dimensionally from Axially
Oriented, Flat Ended Cylinder Specimens in
Low Density Hypersonic Air Flows; Theory
Curves for Continuum Adjusted to Correlate
Directly with Experimental Data

| Theoretical Mass Loss Rate Curves | | | | | |
|---|---|---|---|---|---|
| Experimental Data Points | | | | | |
| Curve No. | Symbol | Nominal $Re_s$ | Model Size, In. | $h_s/RT_o$ | Nozz. Exit, In. |
| (1) | ▲ | 44 | 1" | 400 | 5.0 |
| (2) | ▽ | 51 | 1" | 160 | 5.0 |
| (3) | ◇ | 342 | 1" | 400 | 1.2 |
| (4) | ⊡ | 11 | 1/4" | 350 | 5.0 |
| (5) | ⊙ | 85 | 1/4" | 350 | 1.2 |
| (6) | ● | 2.7 | 1/16" | 350 | 5.0 |

FIGURE 15

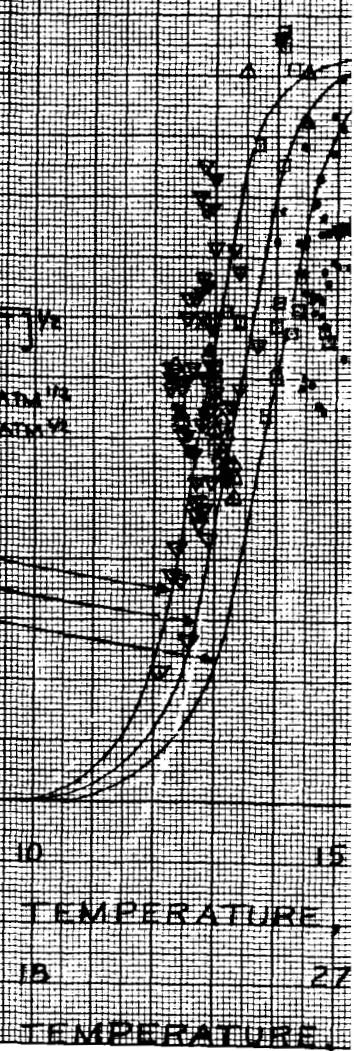OXIDATION MASS RATE VS. SURFACE
TEMPERATURE FOR ATJ GRAPHITE

Data Obtained one-dimensionally from Axially
Oriented Flat Ended Cylinder Specimens in
Low Density Hypersonic Air Flows; Data Ad-
justed for Correlation with Continuum Theory.

$$\dot{m}_w \sqrt{\frac{R_B}{P_e}} = \frac{k_o \, e^{-E/RT}}{[1/k_1 + (k_o/c)^2 e^{2E/RT}]^{1/2}}$$

WHERE $c = 6.2 \times 10^{-3}$ LB/FT$^{3/2}$-SEC-ATM$^{1/2}$

$k_o = 4.42 \times 10^5$ LB/FT$^2$-SEC-ATM$^{1/2}$

$E = 44000$ CAL

$R = 1.987$ CAL/°K

COMPUTED FROM THEORY $\begin{cases} d = 1.0" \\ d = 1/4" \\ d = 1/16" \end{cases}$

WHERE $R_B = \left(\frac{8.45}{24}\right)d$

**DATA KEY**

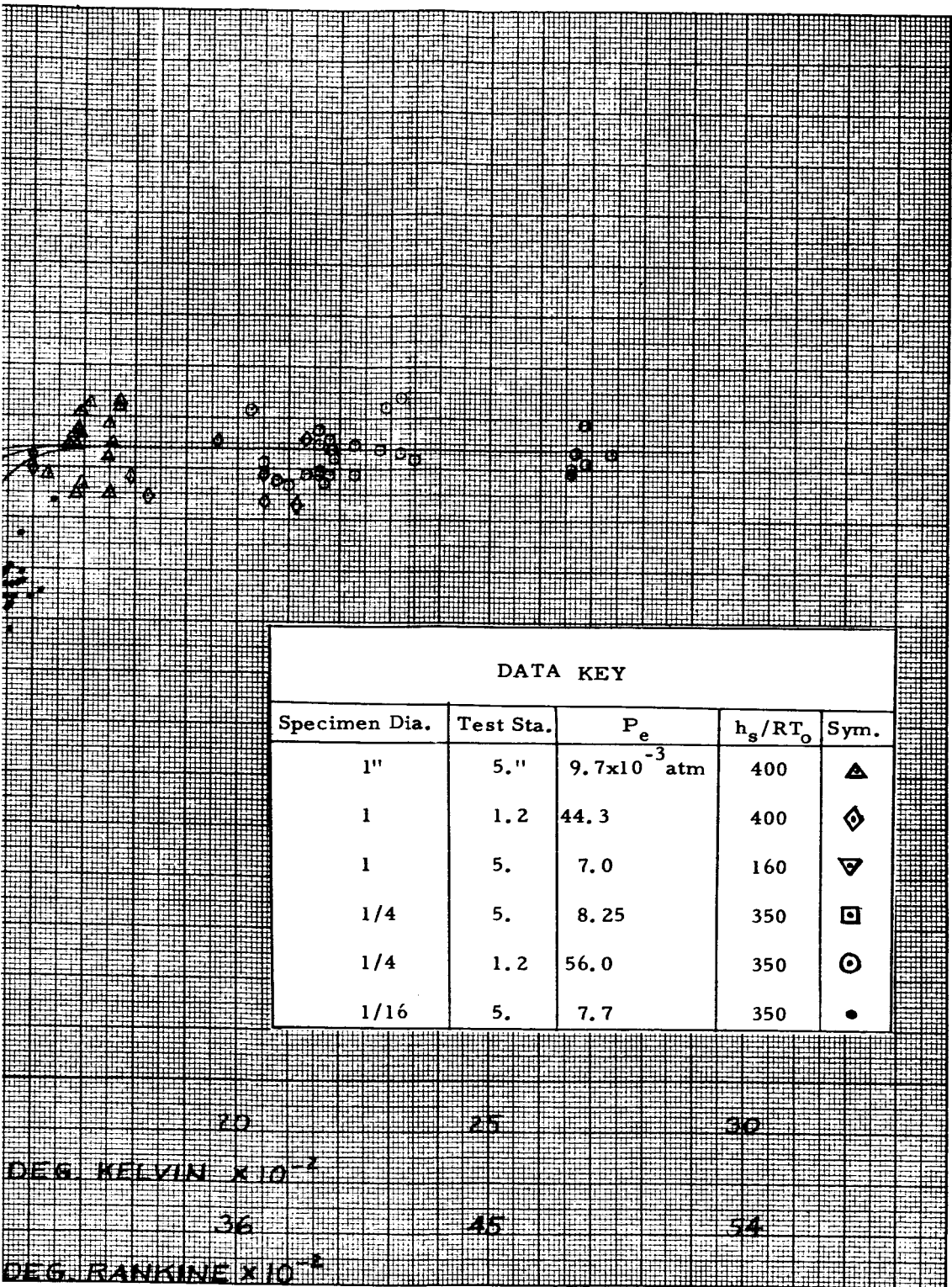| Specimen Dia. | Test Sta. | $P_e$ | $h_s/RT_o$ | Sym. |
|---|---|---|---|---|
| 1" | 5." | $9.7 \times 10^{-3}$ atm | 400 | ▲ |
| 1 | 1.2 | 44.3 | 400 | ◈ |
| 1 | 5. | 7.0 | 160 | ▽ |
| 1/4 | 5. | 8.25 | 350 | ▣ |
| 1/4 | 1.2 | 56.0 | 350 | ⊙ |
| 1/16 | 5. | 7.7 | 350 | • |

DEG. KELVIN $\times 10^{-2}$
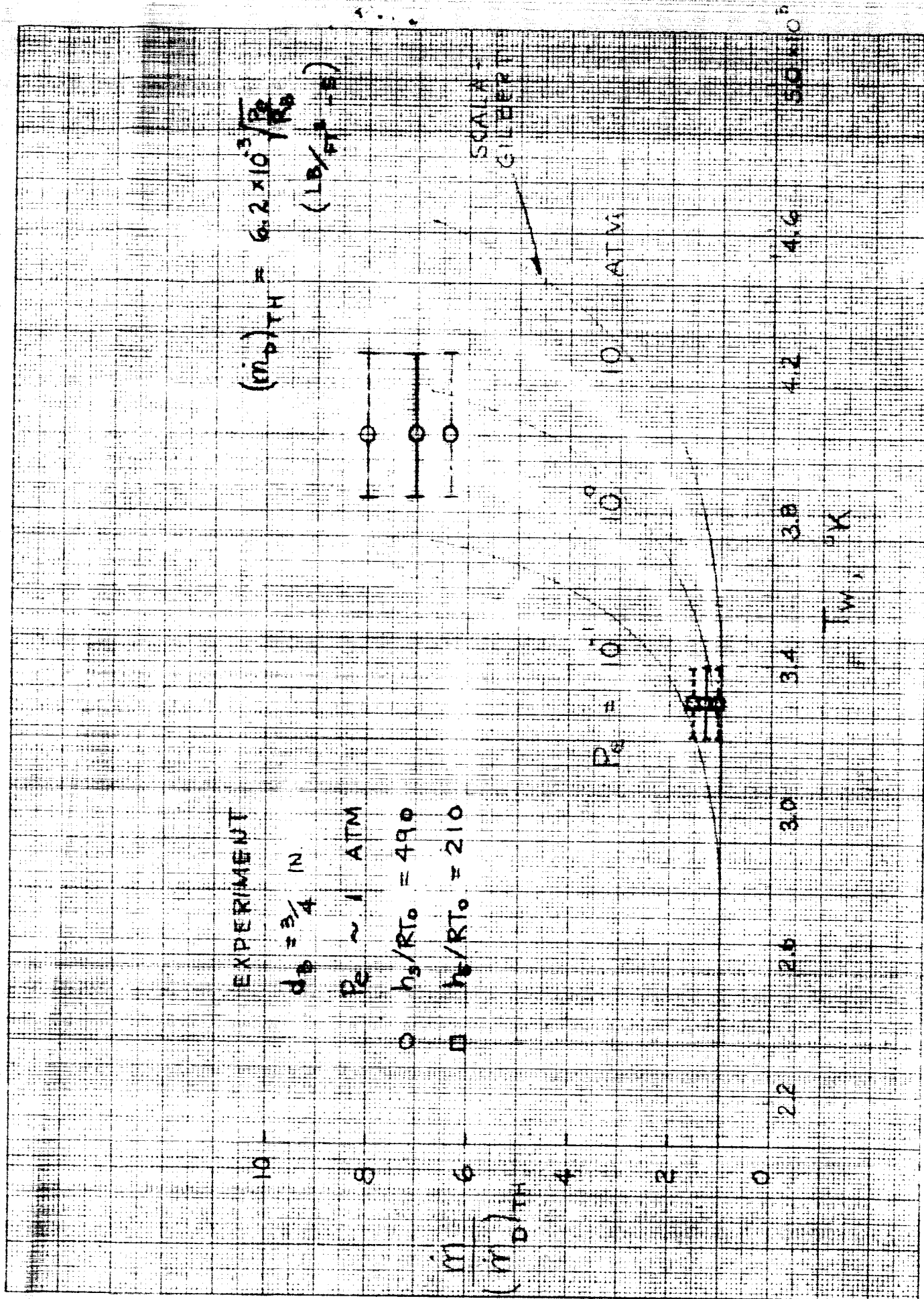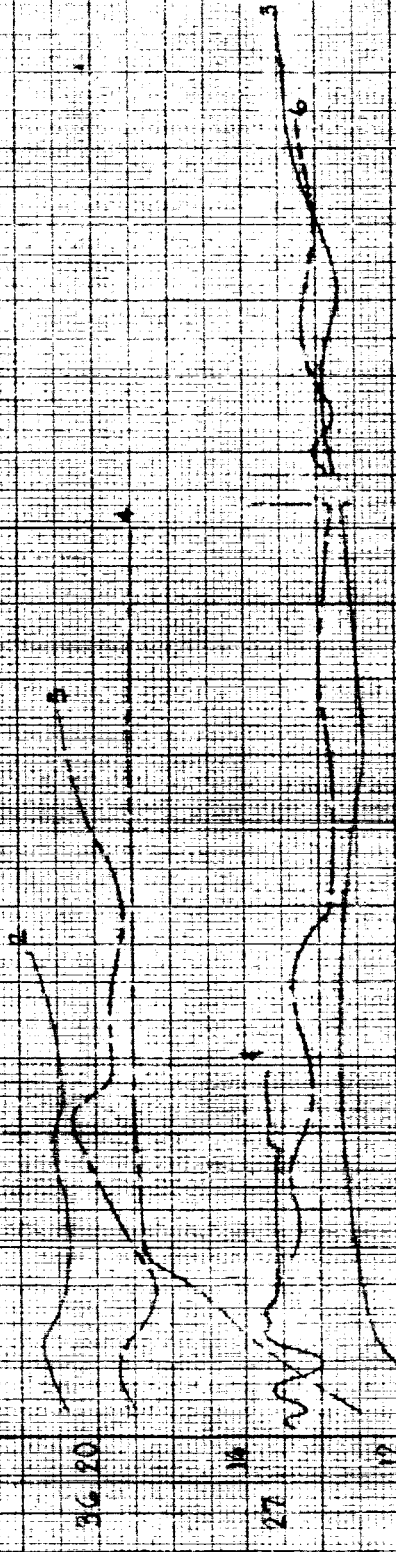
DEG. RANKINE $\times 10^{-2}$

FIGURE 16

FIG. 17   COMPARISON OF EXPERIMENT WITH
THEORY — PYROLYTIC GRAPHITE

RANDOM SELECTION OF
TYPICAL SURFACE TEMPERATURES

CYLINDRICAL MASS RATE SPECIMENS

| CURVE NO. | RUN NO. | MATL | NOMINAL h./sec. | DIA. in. | NOZZLE exit in. |
|-----------|---------|------|-----------------|----------|-----------------|
| 1 | 519 | ATJ | 350 | 1/16 | 5.0 |
| 2 | 497 | " | " | 1/4 | 1.2 |
| 3 | 632 | " | 140 | 1 | 5.0 |

TEMPERATURE

TIME - SECONDS